Since January 2020 Elsevier has created a COVID-19 resource centre with free information in English and Mandarin on the novel coronavirus COVID-19. The COVID-19 resource centre is hosted on Elsevier Connect, the company's public news and information website.

CHAPTER **21**

Radiographic Signs of Joint Disease in Dogs and Cats

Graeme Allan • Sarah Davies

Most radiographic signs of joint disease are nonspecific (Box 21.1, Fig. 21.1). Also, animals with progressive joint disease may have different signs when examined during different phases of the disease. Sound knowledge of joint pathophysiologic characteristics is as important in the diagnosis of joint disease as the ability to make and interpret radiographs of joints.

RADIOGRAPHIC SIGNS OF JOINT DISEASE

Increased Synovial Volume

Any moderate increase in joint capsular or intracapsular soft tissue volume may be detected on good-quality radiographs. The joint cartilage, synovial fluid, synovial membrane, and joint capsule cannot be differentiated, because they are all of soft tissue opacity and therefore silhouette with one another. In most joints, an increase in synovial mass appears as periarticular soft tissue swelling, which is identified radiographically by the increased opacity of affected soft tissues.

In the stifle, the infrapatellar fat pad sign may be used to evaluate synovial volume. The normal infrapatellar fat pad is identified readily on lateral stifle radiographs as a relatively radiolucent triangular region immediately caudal to the patellar ligament (Fig. 21.2). When stifle synovial mass increases, either from increased synovial fluid or soft tissue, a combination of inflammatory response and effusion causes the shape of the fat pad to be altered and the fat pad to become less visible.

Box • **21.1**

Radiographic Signs of Joint Disease

Increased synovial volume
Compressed infrapatellar fat pad
Altered thickness of the joint space
Decreased subchondral bone opacity
Increased subchondral bone opacity
Subchondral bone cyst formation
Altered perichondral bone opacity
Perichondral bony proliferation
Mineralization of joint soft tissues
Intraarticular calcified bodies
Joint displacement or incongruency
Joint malformation
Intraarticular gas

Altered Thickness of the Joint Space

The joint space is the region of soft tissue opacity between subchondral bone surfaces of opposing weight-bearing surfaces of a joint. This space consists of two layers of articular cartilage separated by a microfilm of synovial fluid. In early joint disease, synovial effusion may cause widening of the joint space. As joint disease progresses, attrition of articular cartilage results in decreased width of the joint space (Fig. 21.3). These changes in joint space width are rarely diagnosed radiographically as a result of small animal patients not being radiographed while bearing weight and also because of inconsistency between the orientation of the primary x-ray beam and joint space.

Decreased Subchondral Bone Opacity and Bone Cyst

Subchondral bone is separated from the synovial fluid by an intact layer of articular cartilage. Any disease that changes the character of synovial fluid, causing the articular cartilage to

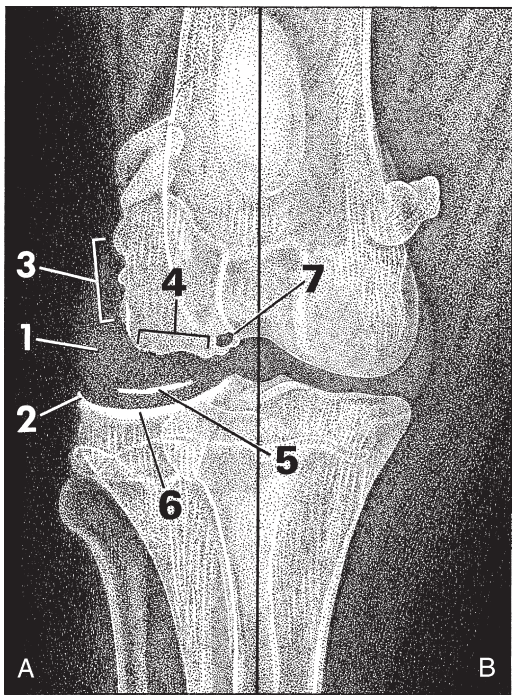

Fig. 21.1 Radiographic signs of joint disease **(A)** compared with a normal joint **(B).** Increased synovial mass *(1)*, perichondral osteophyte *(2)*, and enthesophyte formation *(3)* are common radiographic changes. Erosion of the subchondral bone surface *(4)* and joint mice *(5)* are less common, whereas increased subchondral bone opacity *(6)* and subchondral bone cyst formation *(7)* are signs of chronic joint disease.

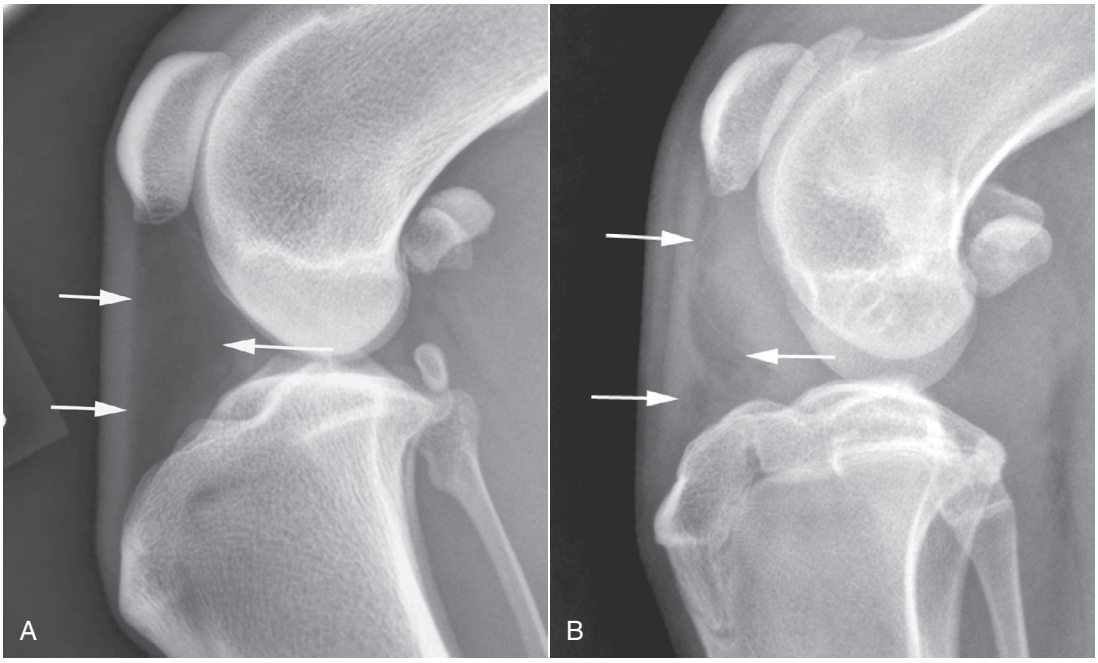

Fig. 21.2 Changes in the shape of the infrapatellar fat pad, located between the *arrows,* is a sensitive indicator of absence **(A)** or presence **(B)** of increased synovial volume in the stifle.

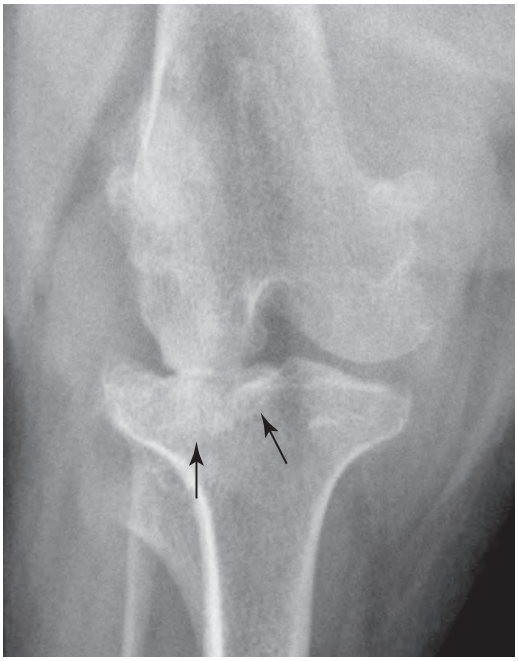

Fig. 21.3 Chronic malalignment of the stifle has resulted in narrowing of the lateral aspect of the femorotibial joint, likely because of degeneration of the lateral meniscus. The secondary altered loading of the lateral tibial condyle has resulted in secondary sclerosis *(black arrows)*.

erode, potentially threatens the integrity of subchondral bone. In inflammatory joint disease, inflammatory exudates may cause pronounced subchondral bone loss. Infectious arthritis may extend into subchondral bone. Subchondral bone loss appears initially as a ragged margin of subchondral bone, but it may extend to cause marked destruction of bone (Fig. 21.4). When bone loss affects smaller carpal and tarsal bones, these small cuboidal bones may be dramatically reduced in mass.

Fig. 21.4 Periarticular soft tissue swelling *(white arrows)* and subchondral bone erosion *(white arrowheads)* in the carpus of a dog with an erosive polyarthropathy. (Courtesy of Perth Veterinary Specialists, Perth, Australia.)

Increased Subchondral Bone Opacity

In benign joint disease, such as degenerative joint disease, subchondral bone may be more opaque than normal because of stress remodeling (see Fig. 21.3). Increased subchondral bone opacity usually appears as a subchondral zone of increased opacity 1 to 2 mm wide.

Altered Perichondral Bone Opacity

Articular cartilage merges with the synovial membrane at the chondrosynovial junction. This highly vascular membrane is sensitive to inflammation. Synovial inflammation, or hypertrophy, may result in erosion of bone adjacent to the synovium.

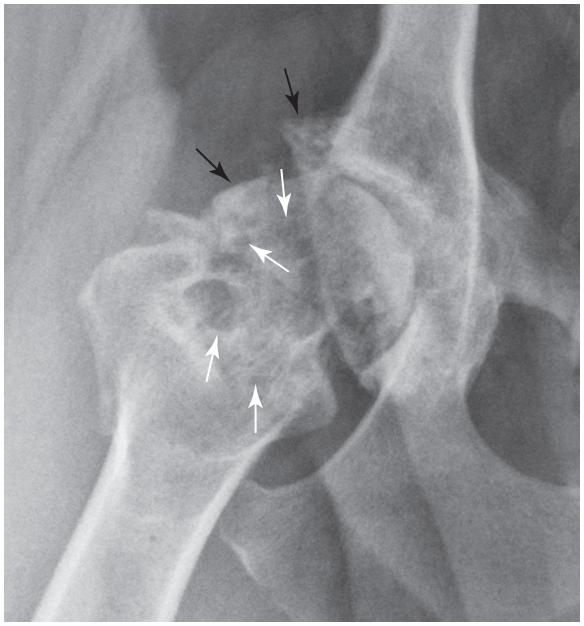

Fig. 21.5 Advanced coxofemoral degenerative joint disease. The femoral neck is thickened, the femoral head is misshapen, and there are numerous osteophytes *(black arrows)*. There are multiple small and large radiolucencies *(white arrows)* in the femoral neck because of invasion of bone by hyperplastic synovium.

Early inflammation causes adjacent bone to appear ragged and spiculated. Longstanding or severe synovial inflammation or hypertrophy may cause pronounced bone erosion (Fig. 21.5).

Articular Soft Tissue Mineralization

Mineralization may occur within the joint capsule, synovial membrane, or synovial fluid as a consequence of chronic joint disease. Occasionally, large accumulations of articular or periarticular calcific material may be observed. Large osteochondromas have been reported within the joints of dogs and cats, and intrameniscal calcification and ossification have been observed in the stifle joints of cats.[1] Pseudogout, or calcium pyrophosphate deposition disease, also causes mineralization of articular and periarticular soft tissues and has been reported in dogs.

Intraarticular Calcified Bodies

Small, well-defined articular and periarticular calcific opacities are occasionally observed in dogs and cats. Such mineralized fragments are sometimes called *joint mice*. Not all such fragments are free within the joint, although they may appear free radiographically; fragments may become adhered to the joint capsule. Articular calcified bodies usually fall into three fairly distinct categories: (1) avulsed fragments of articular or periarticular bone, (2) osteochondral components of a disintegrating joint surface, or (3) small synovial osteochondromas (Table 21.1).[2] They must be differentiated from sesamoid bones.

Joint Displacement or Incongruency

When the normal spatial relation between components of a joint is disturbed, some type of displacement has occurred. A good example is a luxated coxofemoral joint. Other less obvious incongruities, such as the cranial drawer sign in a stifle with a ruptured cranial cruciate ligament and minor elbow incongruity in dogs with elbow dysplasia, can be difficult to see radiographically.[3]

Table • 21.1

Some Common Causes of Calcified Intraarticular Bodies*

JOINT	ETIOLOGY
Shoulder	Osteochondritis dissecans (OCD) of the head of the humerus
	Mineralization of the bicipital tendon/sheath
	Synovial osteochondroma
	Separate centers of ossification on the glenoid rim
Elbow	Ununited anconeal process
	Fragmented coronoid process
	OCD of the humeral medial condyle
Hip	Avulsion epiphyseal fractures after femoral luxation
	Avascular necrosis of the femoral head
Stifle	OCD of the femoral condyles
	Avulsion fractures of the:
	Origin of the long digital extensor tendon
	Origin or insertion of the cruciate ligaments
	Origin of the popliteus
	Meniscal calcification
	Synovial osteochondroma
	Fragmented or fractured sesamoid bones
Tarsus	OCD of the talus

*In all joints, soft tissue periarticular mineralization may occur as a result of degenerative joint disease.

Osteophytes

The proposed pathogenesis of osteophyte formation is that abnormal joint cartilage loading leads to cartilage wear, fibrillation, and loss of cartilage. The products of cartilage degradation mediate synovial hyperplasia and subsequent development of osteophytes.[4] Initially, osteophytes consist of cartilage and later become radiographically visible when they become ossified. They are seen as bony outgrowths at the periphery of articular cartilage. They occur as a component of degenerative joint disease (see Fig. 21.5).

Entheses and Enthesophytes

An enthesis is the point of insertion of a tendon, ligament, joint capsule, or fascia to bone. During embryogenesis ligaments and tendons are attached to cartilage, but subsequent metaplasia of fibroblasts at their attachment site results in formation of fibrocartilage. This extends into the tendon or ligament, and endochondral ossification proceeds within the remaining cartilage. Enthesitis is inflammation of the site of tendon or ligament attachment to bone. An enthesophyte is a bony spondylopathy that develops at an enthesis (Fig. 21.6).[5]

Because enthesophytes, osteophytes, and ankylosing spondylopathy appear radiographically similar, confusion in terminology often occurs when referring to these structures on a radiograph. To separate osteophytes around or within joints from enthesophytes, knowing the location of the common entheses is useful information (Figs. 21.7, 21.8, and 21.9). In complex joints such as the carpus and tarsus, a large number of intraarticular ligaments are present. Every diarthrodial joint has a joint capsule, and intraarticular and periarticular ligaments and joint capsules insert onto bone at their respective entheses. New bone formations arising in or around joints where no known entheses are present are usually referred to as *osteophytes*.

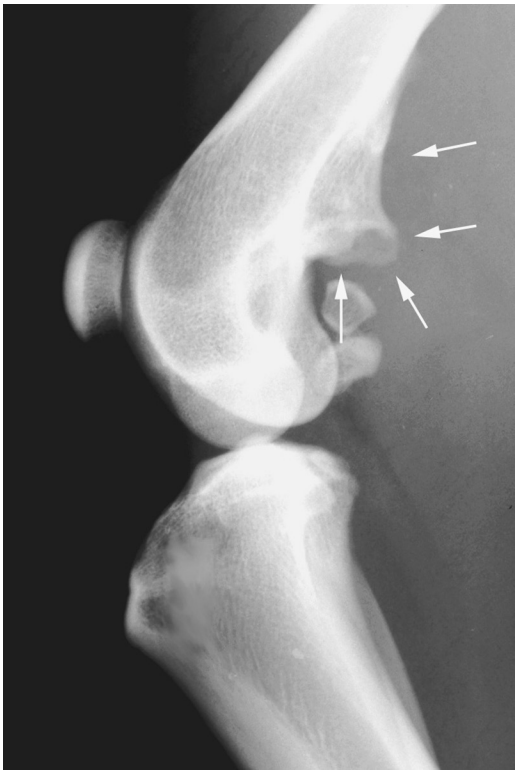

Fig. 21.6 A large enthesophyte arising from the enthesis of origin of the gastrocnemius muscle *(arrows)*.

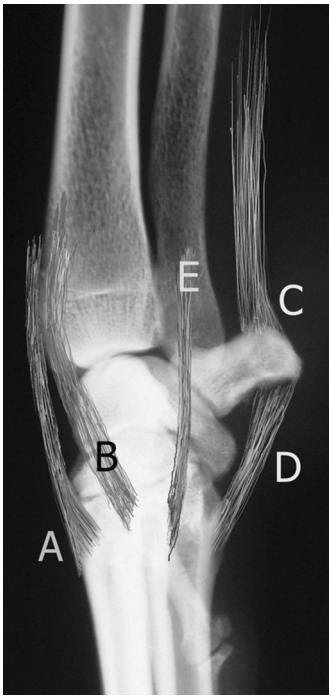

Fig. 21.8 Entheses around the carpus. In addition to the many intraarticular ligaments and the joint capsule (not depicted) are periarticular entheses of extensor carpi radialis and extensor carpi ulnaris *(A)*, abductor pollicis longus *(B)*, flexor carpi ulnaris *(C)*, the check ligaments of the accessory carpal bone *(D)*, and flexor carpi radialis *(E)*.

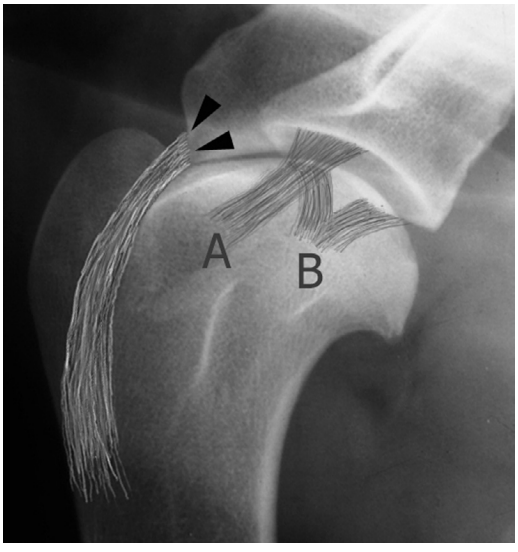

Fig. 21.7 In the scapulohumeral joint the intraarticular tendon of origin of biceps brachii muscle arises from its enthesis *(black arrowheads)* on the scapular tuberosity. Other entheses around the shoulder are related to the lateral *(A)* and medial *(B)* glenohumeral ligaments and the joint capsule and tendons of insertion of supraspinatus, infraspinatus, and subscapularis muscles (not depicted).

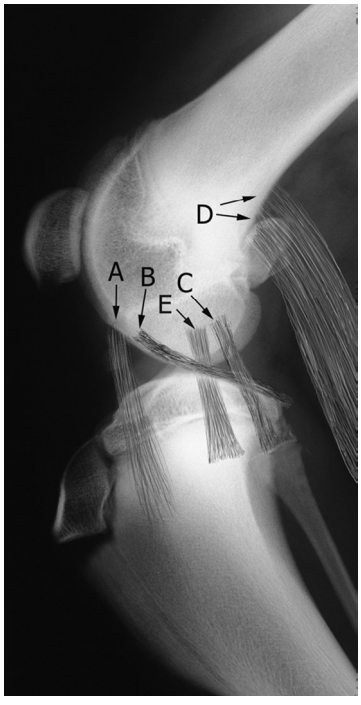

Fig. 21.9 The stifle. Entheses of origin of the long digital extensor *(A)*, popliteus *(B)*, lateral collateral ligament *(C)*, gastrocnemius *(D)*, and medial collateral ligament *(E)*. Not depicted are the cranial and caudal cruciate ligaments.

Intraarticular Gas

Spontaneous or induced gas diffusion into a joint, termed the *vacuum phenomenon*, has been reported in both horses and dogs.[6-10] It has also been observed within the intervertebral disc spaces of dogs at sites of disc prolapse. The presence of intraarticular gas is identified more easily during computed tomography (CT) examinations than during radiography.[9] Current theory is that noniatrogenic intraarticular gas represents diffusion of nitrogen from extracellular fluid into an adjacent joint space when negative pressure is present in the joint. This may occur naturally or be induced by applying traction to a joint. Vacuum phenomenon has many causes in dogs and cats (Box 21.2) and is observed when excessive distraction is applied

Box • 21.2

Causes of Intraarticular Gas

Iatrogenic
After arthrotomy/arthroscopy
Negative-contrast arthrography
Arthrocentesis
Tension on joints
PennHIP distraction radiography
Positioning shoulders with OCD for radiography

Trauma
Joint luxation
Penetrating injuries

Infection
Gas-producing microorganisms

Spontaneous
Intervertebral disc disease
Osteoarthritis
OCD, Osteochondritis dissecans.

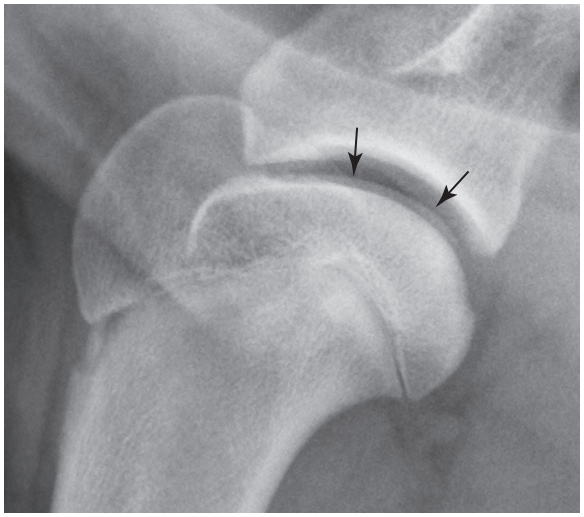

Fig. 21.10 Intraarticular gas is present in the shoulder joint of a dog with osteochondrosis; note the flattening of the caudal aspect of the humeral head. The gas itself is not very conspicuous, but its presence has reduced the opacity of the joint space leading to visualization of the articular cartilage *(black arrows)* If intraarticular gas were not present, the cartilage would not be visible.

to the coxofemoral joints during distraction radiography and has been reported in 20% of shoulder radiographs in dogs with osteochondritis dissecans (OCD) of the humeral head.[7,8] Gas diffusion is likely induced by traction while positioning the shoulder for OCD examination. Interestingly, gas diffusion was not a feature of normal (non-OCD) contralateral joints of dogs in this series.[7] Positive clinical associations with intraarticular gas include degenerative disc disease, cervical vertebral instability, osteochondrosis, and degenerative joint disease (Fig. 21.10). Intraarticular gas diffuses slowly out of a joint over several hours after normal intraarticular pressure is reestablished.

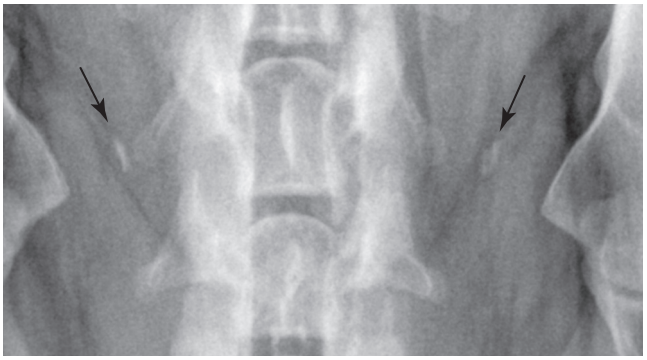

Fig. 21.11 Clavicular remnant medial to the scapulohumeral joints of a dog.

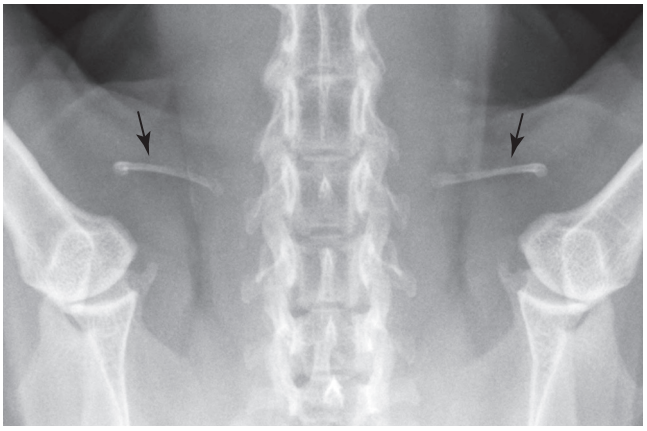

Fig. 21.12 Feline clavicle *(arrows)*.

SESAMOID BONES

Sesamoid bones are located adjacent to the elbow, stifle, tarsus, and the metacarpophalangeal and metatarsophalangeal joints. If sesamoid bones are not identified on a radiograph, they may be absent or be cartilaginous at the time of radiography. The clavicle is present in up to 96% of large dogs and in all cats, but the sesamoids in the iliopubic cartilage were identified in only 11% of one group of greyhounds. In the same group of dogs, the elbow sesamoid, located in the tendon of origin of the supinator, had an incidence of 31%, the lateral plantar tarsometatarsal sesamoid 50%, and the intraarticular tarsometatarsal sesamoid 27%, whereas the popliteal sesamoid is ossified in 84% to 94% of dogs. Sesamoid bones are identified by their size, shape, and location (Figs. 21.11 to 21.18, Table 21.2). Occasionally, displaced sesamoids are regarded as a sign of muscular or tendinous injury. Although this may be true and has been reported in conjunction with ruptured cruciate ligaments and trauma of the tendon of origin of the popliteus and gastrocnemius,[11] variations in sesamoid location may also occur in the absence of a pathologic condition.

Meniscal Ossicles in Cats

Meniscal mineralization is a common finding in domestic cats (Fig. 21.19). In examining stifle radiographs of 100 cats, 46 had meniscal mineralization detected in one or both stifles.[12] Pain scores were not significantly different between stifles with meniscal mineralization and those without. Thirty-four of 57 cadaver stifles had meniscal mineralization, which was always located in the cranial horn of the medial meniscus. Percentage mineralization of the menisci was significantly correlated with cartilage damage in the medial femoral and tibial condyles.

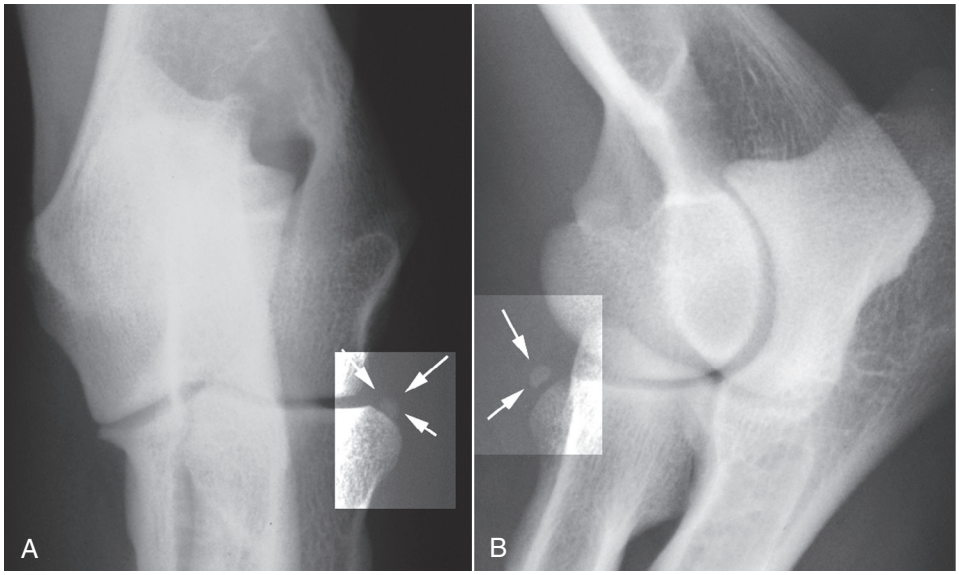

Fig. 21.13 A and B, The elbow sesamoid, in the tendon of origin of the supinator, is seen adjacent to the craniolateral surface of the head of the radius *(arrows)*.

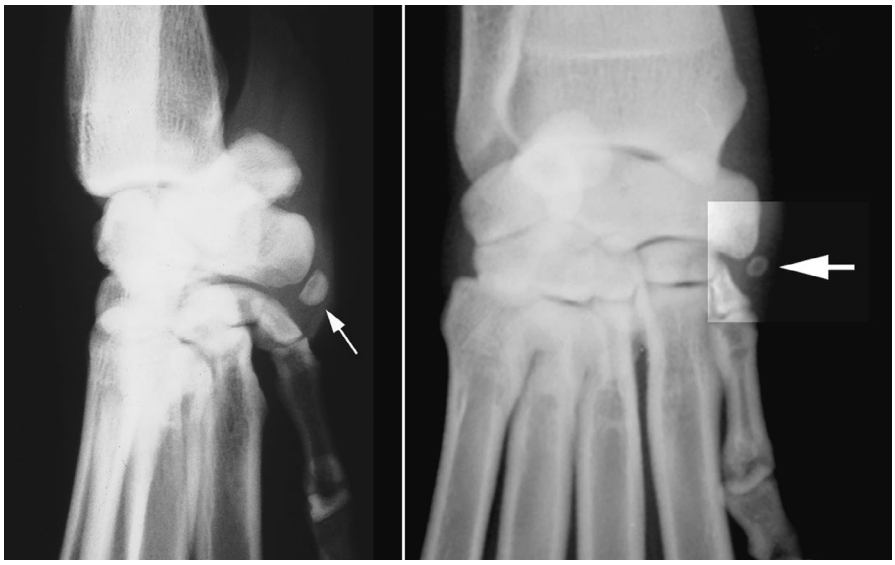

Fig. 21.14 The carpal sesamoid is located in the tendon of the abductor pollicis longus on the medial side of the carpus at the level of the intercarpal articulation *(enhanced box, large arrow)*. The tendon inserts onto the proximal end of the first digit. (Reprinted from *BSAVA manual of canine and feline musculoskeletal imaging*, Quedgeley, Gloucester, England, 2006, BSAVA Publications.)

Therefore, feline meniscal mineralization can be associated with medial compartment degenerative joint disease.[12]

A meniscal ossicle is also a common finding in large nondomestic cats, such as lions, where it is also located in the cranial horn of the medial meniscus.[13]

CONTRAST RADIOGRAPHY OF JOINTS

Radiographs with added contrast medium, either air- or water-soluble iodinated contrast medium, can be used to enhance visualization of intraarticular structures, such as articular cartilage and synovium. Contrast radiography can be used to evaluate the canine shoulder for evidence of osteochondrosis and to identify cartilage flaps. Other applications of contrast arthrography could include evaluation of capsular trauma, documentation of synovial hypertrophy, and identification of radiolucent-joint mice.[14-16] Arthrography has been largely replaced by CT and magnetic resonance imaging (MRI).

SESAMOID DISEASE

A syndrome of metacarpophalangeal sesamoid bone fragmentation has been reported in several large breeds of dogs but occurs most commonly in rottweilers.[16] The underlying cause appears to be osteonecrosis of selected sesamoids, although developmental, traumatic, and degenerative conditions are possible. Eight palmar/plantar sesamoids are present on the four main digits of each of the manus or pes, but sesamoid fragmentation affects mainly the second and seventh palmar sesamoid bones (Fig. 21.20). The incidence has been reported

Fig. 21.15 The metacarpophalangeal and metatarsophalangeal sesamoids are paired *(white arrowheads)* on the palmar (plantar) surface and single on the dorsal surface *(white and black arrows)*. They are numbered from medial to lateral. (Reprinted from *BSAVA manual of canine and feline musculoskeletal imaging*, Quedgeley, Gloucester, England, 2006, BSAVA Publications.)

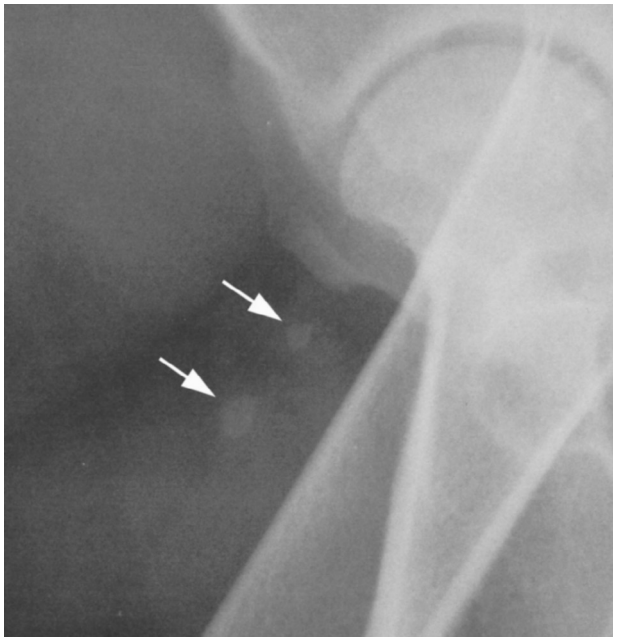

Fig. 21.16 The iliopubic sesamoids are occasionally seen cranial to the pubic eminence on lateral radiographs of the pelvis of large dogs *(white arrows)*.

to be as high as 44% in one group of rottweilers. In another group of 55 rottweilers, radiographic incidence of sesamoid disease at 12 months old was 73%, with an incidence of clinical signs attributable to sesamoid disease in 65% of affected dogs. Sesamoid disease was identified as the cause of forelimb lameness in 50% of young rottweilers.[17]

Dorsopalmar radiographs usually allow identification of affected sesamoid bones, but oblique lateral projections with the digits separated by traction may provide additional information. Radiographically, fragmented sesamoid bones appear as a cluster of ossific fragments on the palmar aspect of the joint, adjacent to an unaffected paired sesamoid. Ossicles are usually multiple, with rounded margins that conform to a variety of shapes and sizes (see Fig. 21.20). In racing greyhounds, clearly defined transverse separation of sesamoid bones have been reported, leading to a belief that fracture is the cause of sesamoid fragmentation in this breed.[18]

Although less frequently affected than sesamoids in the manus, fabellae are also prone to fragmentation (Fig. 21.21).

The most common example of sesamoid displacement is medial luxation of the patella (Fig. 21.22). Patella luxation occurs most frequently in toy dogs and also in Devon rex cats. Some breeds have an inherited predisposition to patella luxation. Other sesamoid bones are also prone to displacement. Distal displacement of popliteal sesamoids or fabellae can indicate rupture or trauma to their respective tendons, although this is not always true (Fig. 21.23).

Degenerative Joint Disease

Degenerative joint disease is a slowly progressive disease of synovial joints in which synovial effusion and cartilage degradation are key components. It is the most common joint abnormality seen in small animal practice and occurs most frequently in the weight-bearing joints of medium-sized to large dogs, although it may affect any synovial joint of both dogs and cats. The best example of canine degenerative joint disease occurs as a result of canine hip dysplasia. The incidence of hip dysplasia varies from breed to breed and exceeds 50% in many large breeds. The next most frequent locations of degenerative joint disease are the canine shoulder and stifle. Signs of shoulder degenerative joint disease were identified in 33% to 50% of groups of dogs surveyed either at necropsy or radiographically;

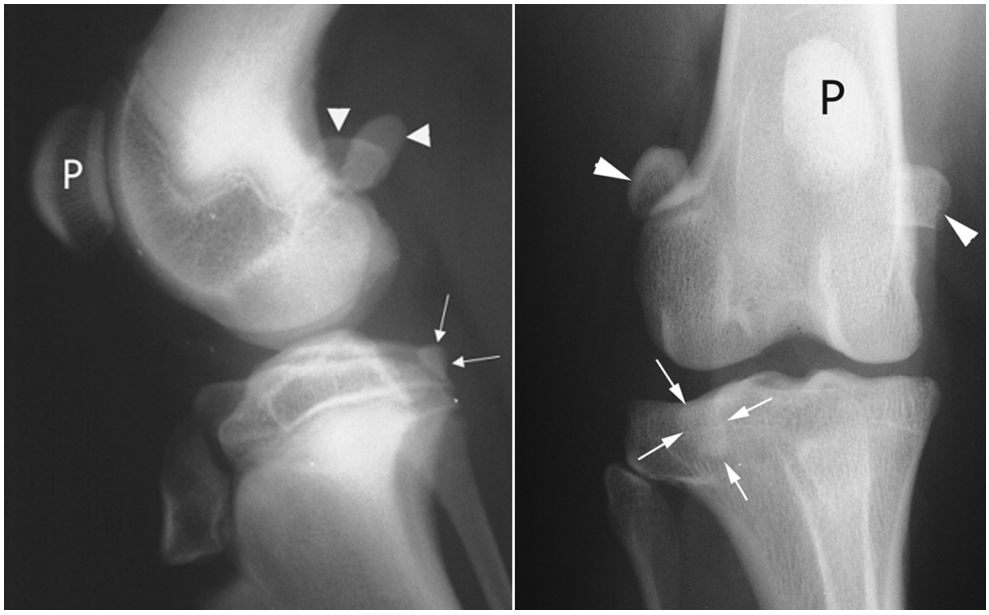

Fig. 21.17 The patella *(P)* is easily identified on the cranial aspect of the femoral condyle. The paired fabellae *(white arrowheads)* are located on the caudal aspect of the femoral condyle, where they lie adjacent to the medial and lateral condyles near the origin of the gastrocnemius. The popliteal sesamoid *(white arrows)* is located caudolaterally, adjacent to the head of the tibia.

Fig. 21.18 The lateral tarsometatarsal sesamoid *(white arrows)* and the medially located intraarticular tarsometatarsal sesamoid *(black arrows)* are inconsistently present in dogs and can be difficult to locate. On the lateral image *(right panel)* one can be seen *(white arrowheads)*. (Reprinted from *BSAVA manual of canine and feline musculoskeletal imaging*, Quedgeley, Gloucester, England, 2006, BSAVA Publications.)

20% of dogs in another survey had evidence of stifle degenerative joint disease at necropsy.[19]

Degenerative joint disease may be a primary aging change (idiopathic) or occur as a result of a developmental or acquired disorder. Examples of canine developmental disorders include osteochondrosis, elbow incongruity leading to fragmented medial coronoid process, ununited anconeal process, hip dysplasia, patellar luxation, achondroplasia, and conformational disorders, such as valgus and varus deformities of the carpus. Acquired disorders capable of causing degenerative joint disease in dogs include trauma, joint instability, epiphyseal aseptic necrosis, recurrent hemarthrosis, and acquired postural or conformational defects, such as joint malalignment after fracture repair.

Radiographic Signs of Progression of Osteoarthritis in Dogs

The stifle is often used to study the progression of canine degenerative joint disease. Initial stages are asymptomatic, and radiographs are usually normal. The first change is mild nonsuppurative synovitis, accompanied by increased synovial mass with alteration of the shape of the infrapatellar fat pad. Focal articular cartilage degeneration follows. The joint space may

Table • **21.2**

Sesamoid Bones Visible on Radiographs of Joints of the Canine

APPENDICULAR SKELETON	JOINT: NAME/LOCATION
Shoulder	Clavicle (medial end of tendinous intersection in the brachiocephalicus) (see Figs. 21.11 and 21.12)
Elbow	Tendon of origin of the supinator (see Fig. 21.13)
Carpus	Tendon of the abductor pollicis longus (see Fig. 21.14)
Metacarpophalangeal	Paired palmar sesamoid bones (located in the tendons of insertion of the interosseous muscles) (see Fig. 21.15)
	Single dorsal sesamoid (located in the extensor tendons)
Coxofemoral	None* (see Fig. 21.16)
Femorotibial	Patella (tendon of insertion of the quadriceps femoris) (see Fig. 21.27)
	Sesamoid bones of the gastrocnemius (fabellae)
	Medial head
	Lateral head
	Popliteal sesamoid (tendon of the popliteus)
Tarsus	Lateral plantar tarsometatarsal sesamoid bone (see Fig. 21.18)
	Intraarticular tarsometatarsal sesamoid bone
Metatarsophalangeal	Paired plantar sesamoid bones (see Fig. 21.15)
	Single dorsal sesamoid bone

*Sesamoid bone located in the iliopubic cartilage may be seen cranial to the iliopubic eminence.

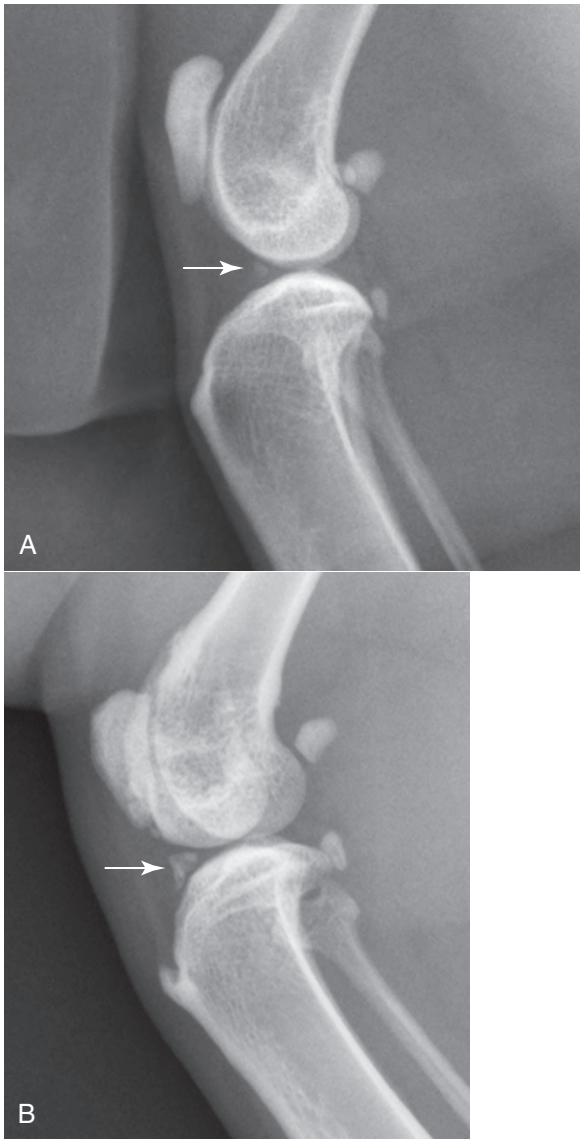

Fig. 21.19 **A,** A small meniscal ossicle in a cat *(white arrow)*. **B,** A moderately sized meniscal ossicle in another cat *(white arrow)*. There is also an enthesophyte at the patellar ligament attachment site on the proximal tibia.

be wider during this stage. As a feature of degenerative joint disease, osteophytosis is progressive and is characterized by the greatest degree of change over time in the canine stifle with naturally occurring instability. When grading stifle degenerative joint disease, evaluating changes in number and size of periarticular osteophytes is more reliable than evaluating subchondral sclerosis, intraarticular mineralization, or synovial effusion, but signs of synovial effusion and compression of the infrapatellar fat pad are identifiable radiographic features that often accompany stifle instability.

Osteophyte formation commences as early as 3 days after cranial cruciate ligament transection and can be seen radiographically at the margins of the femoral trochlea as early as 2 weeks after the onset of stifle instability. Initially, osteophytes consist of cartilage, and they do not become visible radiographically until they are ossified. Proximal and distal ends of the trochlear ridges are the earliest sites of osteophyte formation in the stifle. At a later stage osteophytes develop on the lateral and medial femoral condylar surfaces and tibial condyles, and the patella. Enthesophytes form at points of origin and insertion of cruciate and collateral ligaments subsequent to trochlear ridge osteophytosis.

Specific radiographic projections, such as flexed mediolateral, craniomedial-caudolateral, and caudomedial/craniolateral radiographs can be used to facilitate early identification of trochlear ridge osteophytes.[4,20]

In the coxofemoral joint, synovial effusion may cause subluxation. The presence of subluxation is a powerful indicator of the risk of development of coxofemoral degenerative joint disease.[21-23] There is a strong correlation between the unitless distraction index (DI), a quantifiable measure of subluxation, and subsequent development of degenerative joint disease. The likelihood of coxofemoral degenerative joint disease varies with breed and with the DI. Interestingly, the threshold DI, below which coxofemoral degenerative joint disease is unlikely to occur, is breed specific. The threshold DI for the German shepherd is 0.3, and it appears higher (0.4) for the Labrador retriever and rottweiler.

Radiographic changes of degenerative joint disease vary according to the stage of disease. The most readily recognizable

Fig. 21.20 A, Fragmentation of sesamoids 4 and 7 of the manus *(arrows)*. **B,** A similar rottweiler *(white arrows)* has concurrent osteitis of the distal end of a metacarpal bone *(black arrowheads)*. **C,** The osteitis was identified as the active lesion using nuclear scintigraphy, and the fragmented sesamoids were not considered clinically significant. (**B** and **C,** Courtesy of Dr. R. M. Zuber, Gladesville Veterinary Hospital, Sydney, Australia.)

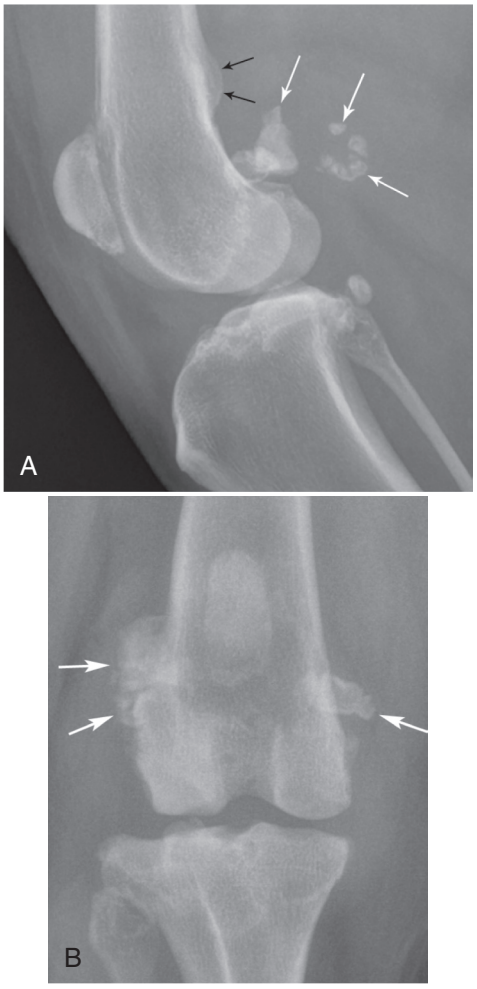

Fig. 21.21 Lateral **(A)** and craniocaudal **(B)** radiographs of a stifle of an adult dog with fragmentation of the fabellae *(white arrows)*. Note enthesopathy *(black arrows)* at the origin of the medial and lateral heads of the gastrocnemius muscle.

change is enthesophyte and osteophyte formation, which follows neovascularization of the chondrosynovial junction with resultant fibrocartilage formation. This fibrocartilage collar gradually ossifies with the formation of perichondral new bone (Fig. 21.24). Enthesophytes develop on non–weight-bearing surfaces and are eventually incorporated into adjacent ligamentous or capsular attachments.[18,19]

Thinning of the joint space is observed rarely (see Fig. 21.3). Pathologic alteration of subchondral bone may be detected as increased subchondral opacity of the weight-bearing surface (see Fig. 21.3). Subchondral cyst formation, a feature of degenerative joint disease of the human femoral head, has also been observed in joints of small animals (see Fig. 21.5).

Affected joints exhibit decreased range of movement, which results in increased loading of the diminished weight-bearing surface. The combination of increased load, diminished subchondral strength, and loss of shock-absorbing cartilage results in altered shape of the subchondral bone table. This remodeling of subchondral bone is complemented by the addition of peripheral new bone in the form of perichondral osteophytes. Altered shape of the osseous components of affected joints is readily identified radiographically. The gamut of radiographic changes seen in degenerative joint disease is outlined in Box 21.3.

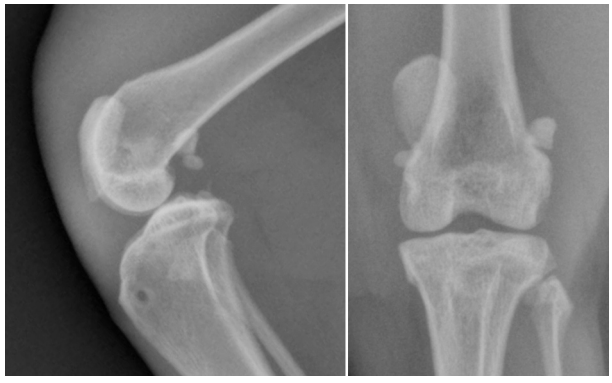

Fig. 21.22 Medial luxation of the patella in a cat associated with complex joint trauma. On the lateral image, the luxated patella is superimposed on the trochlea of the femoral condyle. (Courtesy of Cremorne Veterinary Hospital, Sydney, Australia.)

Osteoarthritis in Cats

Osteoarthritis is common in domestic cats.[24] Primary causes of articular cartilage degeneration and consequent degenerative joint disease in cats include the storage disease mucopolysaccharidosis (MPS) and osteochondral dysplasia of Scottish fold cats. Established secondary causes of feline degenerative

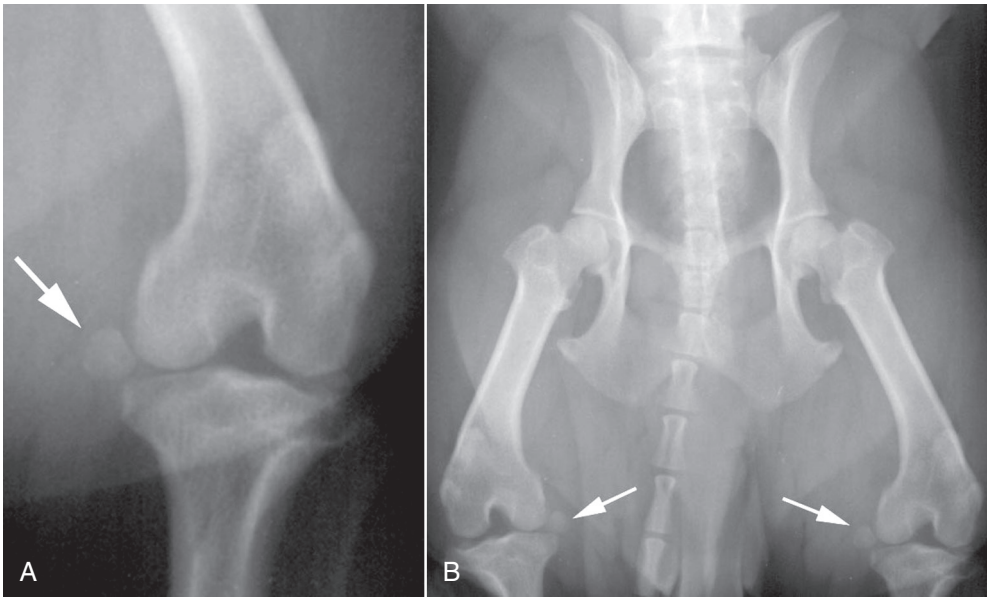

Fig. 21.23 **A,** Distal displacement of the medial fabella *(white arrow)* of the left stifle of a 2-year-old male West Highland white terrier. This may be associated with rupture of the medial head of the gastrocnemius muscle, but this abnormality was bilaterally symmetric (**B,** *white arrows)*. In this circumstance, distal displacement of the medial fabellae is unlikely to be clinically significant and is most likely a normal variant. (Courtesy of University Veterinary Centre, Sydney, Australia.)

Fig. 21.24 **A** and **B,** A 7-year-old German shepherd dog had chronic weight-bearing lameness of the right pelvic limb. Perichondral osteophytes and enthesophytes are visible on the distal femur and proximal tibia. Synovial effusion is also present. **C** to **E,** Osteoarthritis in the elbow of a 2-year-old German shepherd. Osteophytes on the cranial aspect of the head of the radius **(C)** and on the medial edge of the coronoid process of the ulna **(D)** and enthesophyte formation on the anconeal process **(E)** are degenerative changes often seen secondary to elbow incongruity and fragmented medial coronoid process.

joint disease (Fig. 21.25) include developmental and traumatic conditions that alter joint stability, as well as dietary (hypervitaminosis A) causes. Many infectious and immune-based arthropathies alter the integrity of articular cartilage, leading to a cascade of articular changes, with degenerative joint disease as the end result. There is poor correlation between radiographic signs of degenerative joint disease in older cats and associated clinical lameness.

Cats with uncomplicated degenerative joint disease may be free of clinical signs of joint disease, and radiographic signs of this condition are often discovered accidentally. Most syndromes listed in Box 21.4 are characterized by recognizable clinical signs that are accompanied by appendicular skeletal pain and lameness.

Radiographic signs of degenerative joint disease in cats are similar to those reported in dogs. Periarticular new bone formation as osteophytes or enthesophytes develops around affected joints (see Fig. 21.25). Although articular cartilage is invisible on survey radiographs, remodeling and increased opacity of subchondral bone adds to the altered joint architecture. Subchondral bone changes usually imply changes in joint cartilage. Signs of synovial effusion and/or thickened periarticular soft tissue are seen less commonly in cats than in dogs, whereas the incidence of intraarticular soft tissue calcification is more common in cats. Other changes that accompany feline degenerative joint disease include intraarticular and periarticular soft tissue calcification, often ascribed to synovial osteochondromatosis, and prolific periarticular osteophytosis.

Box • 21.3

Radiographic Signs of Degenerative Joint Disease

Synovial Effusion
Initial widening, then thinning, of the radiolucent joint space
Perichondral enthesophyte formation of non—weight-bearing surfaces
Increased subchondral bone opacity
Remodeling of subchondral bone
Mineralization of intraarticular and periarticular soft tissues
Subchondral cyst formation

Box • 21.4

Causes of Osteoarthritis in Cats

Primary
Scottish fold osteochondrodysplasia
Mucopolysaccharidosis (MPS)
Age-related cartilage degeneration

Secondary
Congenital
Hip dysplasia
Trauma
- Traumatic joint instability
- Physeal fractures

Infectious/inflammatory
- Viral (calicivirus, coronavirus)
- Bacterial (bacterial L-form, mycoplasma, bite wounds)
- Fungal (cryptococcosis, histoplasmosis)

Nutritional
- Hypervitaminosis A

Immune mediated
- Rheumatoid arthritis
- Progressive proliferative polyarthropathy

Systemic lupus erythematosus (SLE)
- Idiopathic polyarthritides

Reprinted from Allan GS: Radiographic features of feline joint diseases, *Vet Clin North Am Small Anim Pract* 30:281, 2000.

Fig. 21.25 Craniocaudal **(A)** and mediolateral **(B)** projections of a feline elbow with marked degenerative joint disease. Exuberant periarticular new bone formation is present around the elbow. (Courtesy of Paddington Cat Hospital, Sydney, Australia.)

HIP DYSPLASIA

Hip dysplasia is abnormal development of the coxofemoral joints. Hip dysplasia occurs principally in large dogs but also affects small dogs and cats. The condition is typically bilateral but can be asymmetric.

Hip dysplasia is an inherited disorder. Heritability estimates range from 0.2 to 0.6. With the use of more sensitive radiographic interpretation and newer methods of imaging the coxofemoral joints, estimated heritability in German shepherd dogs has been raised from 0.46% to 61%.[25] Environmental factors influence the phenotypic expression of hip dysplasia. Overnutrition is one of the principal nongenetic factors that influences expression of canine hip dysplasia.[26] Hip dysplasia is a developmental, age-related disorder; and the phenotypic manifestations are not present at birth. A variable amount of time must elapse before radiographic changes manifest. Once present, these radiographic changes usually progress with age.

The earliest recognizable changes in the coxofemoral joints are a combination of perifoveal cartilage erosion, hypertrophy of the round ligament of the femoral head, synovial effusion, and synovitis.[27] These changes cannot be identified radiographically, but the strongest clue to their presence can be obtained by testing for signs of joint laxity, which appears to be precipitated by synovial effusion. Joint laxity may be palpated and visualized radiographically (Figs. 21.26 and 21.27).[28,29] Subsequent radiographic changes are those of degenerative joint disease (Fig. 21.28) developing as (1) perichondral osteophyte formation, (2) remodeling of the femoral head and neck, (3) remodeling of the acetabulum, and (4) increased opacity of subchondral bone of the femoral head and acetabulum. A line of enthesophytes on the caudal aspect of the femoral neck, termed the *Morgan line,* has been described as an early sign of coxofemoral degenerative joint disease (Fig. 21.29).[30] As the degenerative process advances, the femoral neck becomes thickened, and the surface of the neck becomes irregular as a result of the growth of a collar of perichondral osteophytes. The acetabulum loses its cuplike shape and becomes shallow. Increased bone opacity of subchondral articular surfaces represents bone sclerosis, which is a response to cartilage thinning. Subchondral cyst formation is an infrequent manifestation of degenerative joint disease in small animals but may be observed occasionally.

Fig. 21.26 Normal mature coxofemoral joint. Note that at least half the femoral head lies medial to the dorsal acetabular margin *(white arrows)*. The cranial margin of the femoral head is separated from the adjacent acetabulum by a fine radiolucent line, which represents the joint cartilage and a microfilm of synovial fluid *(black arrows)*. The shape of the radiolucent joint space is symmetric.

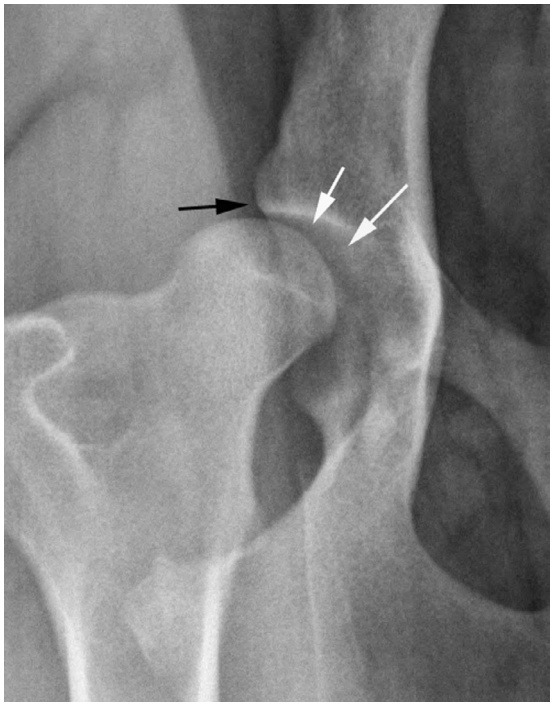

Fig. 21.27 Moderate hip dysplasia. Subluxation of the femoral head is accompanied by remodeling of the acetabulum. The cranial acetabular margin is angulated *(black arrow)*, and the acetabulum is shallow. Note the wedge-shaped joint space *(white arrows)* created by subluxation of the femoral head.

Fig. 21.28 Moderate coxofemoral degenerative joint disease. The acetabulum and the femoral head have undergone advanced remodeling. Osteophytes have formed on the femoral neck and head, as well as on the cranial acetabular margin. New bone formation has filled the acetabular fossa, and the opacity of acetabular subchondral bone is increased.

The incidence of hip dysplasia in domestic shorthaired cats, based on standard hip radiography, has been estimated at 6.6%.[31] The incidence is higher in purebred cats (12.3%), with some breeds, such as the Maine coon cat, having an incidence of 18% to 21%.[31] When passive coxofemoral laxity is evaluated by stress radiography, the overall incidence of feline hip dysplasia may be as high as 32%. The prevalence of feline hip dysplasia is lower than the prevalence in dogs.

Radiographic criteria for diagnosing feline hip dysplasia include the presence of signs of coxofemoral subluxation (Fig. 21.30), enthesophyte formation on acetabular margins, and remodeling and degenerative changes of the femoral head and neck (Fig. 21.31). Unlike canine hip dysplasia, most degenerative changes in cats appear on the craniodorsal acetabular margins, with a low incidence of degenerative remodeling reported on the femoral head and neck.

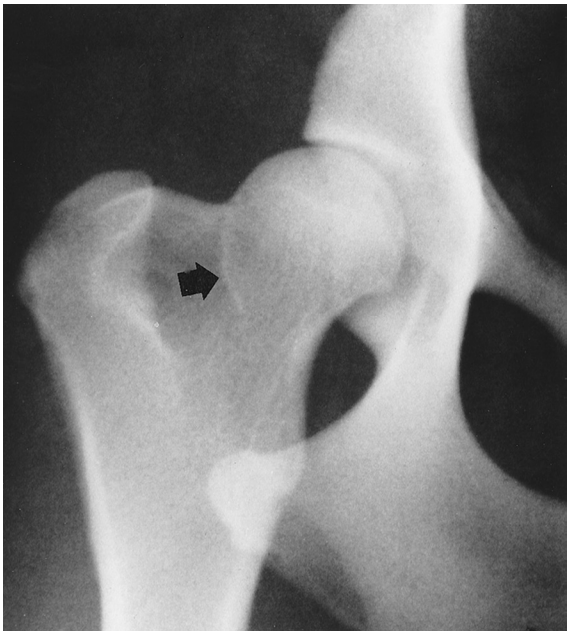

Fig. 21.29 An early sign of degenerative joint disease is the Morgan line, representing enthesophyte formation on the caudal aspect of the femoral neck, medial to the trochanteric fossa *(black arrow)*.

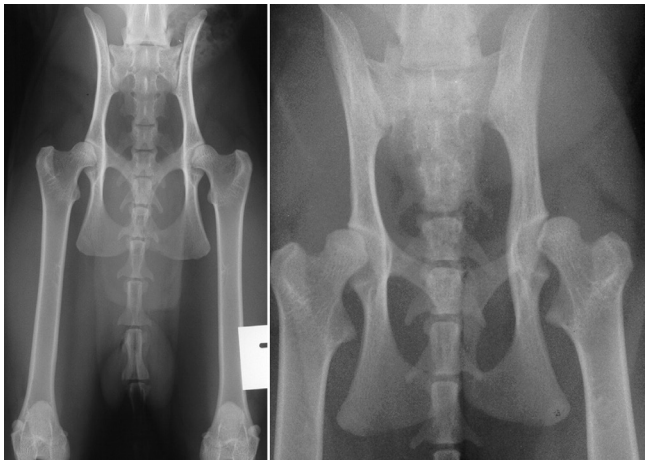

Fig. 21.30 Feline coxofemoral joints. **A,** Normal. **B,** Abnormal with coxofemoral subluxation. (**B,** Courtesy of University Veterinary Centre, Sydney, Australia.)

Methods of evaluating the coxofemoral joints can be divided into those that identify joint laxity proactively and those that examine for radiographic evidence of degenerative joint disease. Phenotypic screening programs used internationally fall into the latter group and rely on assessment of the extended ventrodorsal radiographic projection (Fig. 21.32A), although this projection is an insensitive indicator of coxofemoral joint laxity. To identify coxofemoral joint laxity reliably, a stressed ventrodorsal projection is used. With the femurs in a distracted position (see Fig. 21.32B), coxofemoral laxity can be quantified and the calculated laxity index (i.e., Distraction Index) used to rank individual dogs within their breed with respect to hip joint tightness or looseness.[32] The Distraction Index (DI) is also a useful indicator of the likelihood of future coxofemoral degenerative changes. This information can be obtained at a much earlier age by using distraction radiography than with the standard extended ventrodorsal projection. Assessing coxofemoral laxity is an important component of complete radiographic assessment of the coxofemoral joints.

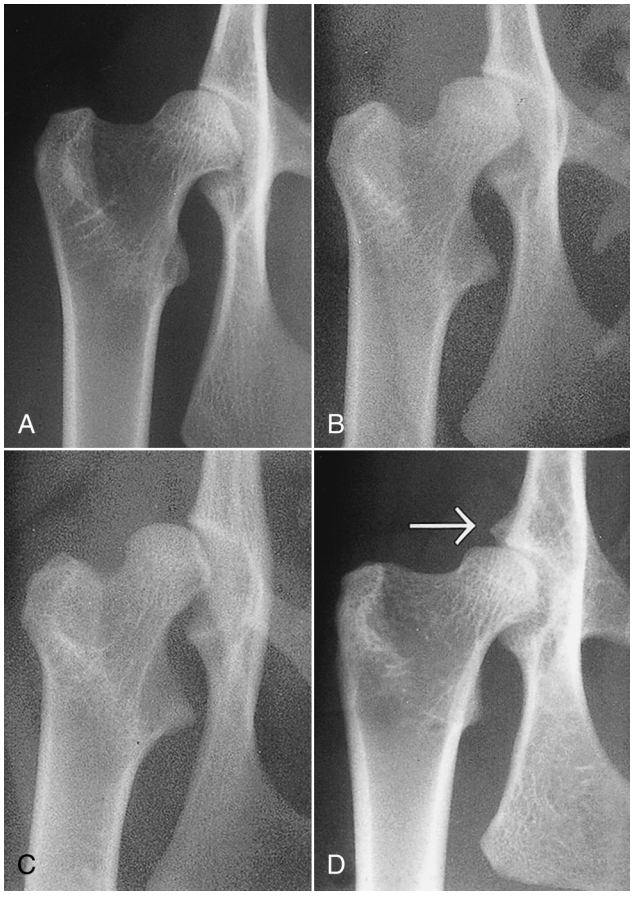

Fig. 21.31 Feline hip dysplasia. **A,** "Normal" is compared with varying degrees of coxofemoral subluxation (**B** and **C**). **D,** Degenerative changes, with osteophyte formation on the cranial effective acetabular margin *(white arrow)*, are a typical manifestation of feline coxofemoral degenerative joint disease. (Reprinted from Allan GS: Radiographic features of feline joint diseases, *Vet Clin North Am Small Anim Pract* 30:281, 2000.)

Many screening programs require that the extended ventrodorsal radiograph of the coxofemoral joints be made and submitted for evaluation. The method of obtaining the extended hip projection, as required by the Orthopedic Foundation for Animals (OFA) for example, is similar to projections used by other screening programs internationally. With the dog in dorsal recumbency, the hind limbs are extended with the femurs parallel and the stifles rotated inward so that the patellae are located over the middle of the cranial surface of the distal femur. The x-ray beam should be centered over the coxofemoral joints, and the radiograph should include the entire pelvis and femurs. The pelvis must appear symmetric in the radiograph, without evidence of rotation (see Figs. 21.30A and 21.32). Failure to anesthetize the subject may decrease radiographic sensitivity for signs of coxofemoral joint laxity. Because the extended ventrodorsal projection is an insensitive method of detecting signs of coxofemoral subluxation,[32] care must be taken to ensure accurate subject positioning and satisfactory radiographic quality.

The PennHIP method[21,22,32] also requires the dog be in dorsal recumbency. Femurs are placed in a neutral position to duplicate standing. This neutral position avoids spiral tensioning of the joint capsule that forces the femoral head into the acetabulum and artificially reduces subluxation, a significant disadvantage of the extended hip projection. Hind limbs are held with the femurs positioned neutrally, and a radiograph is made while the coxofemoral joints are compressed to obtain an image of

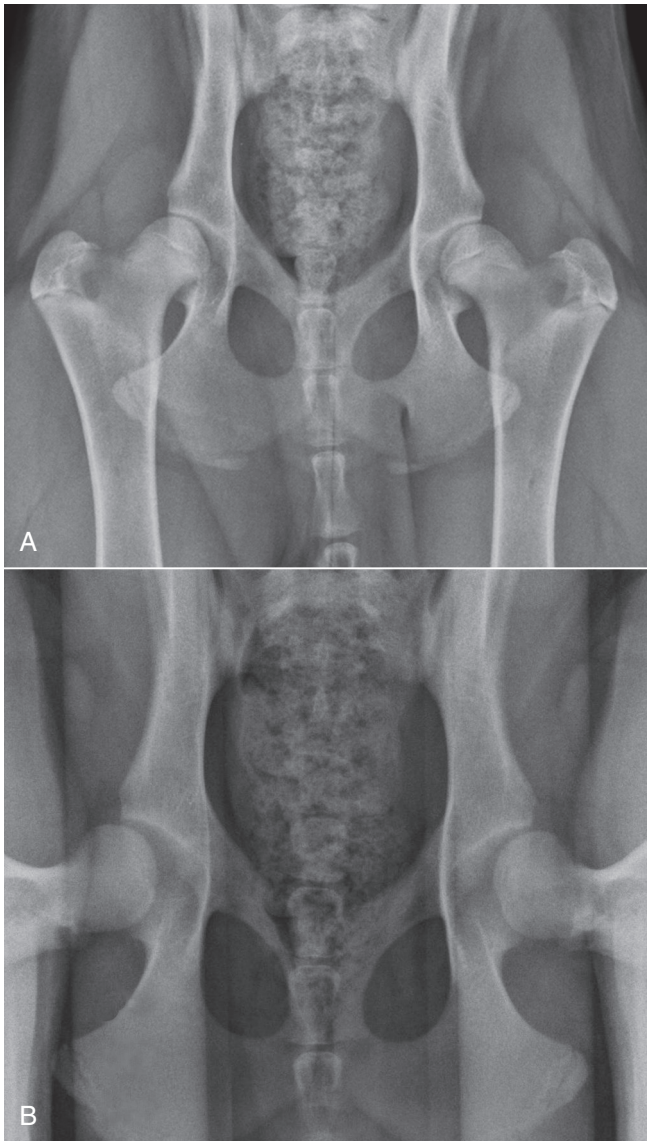

Fig. 21.32 **A,** Extended ventrodorsal projection of the coxofemoral joints (Orthopedic Foundation for Animals [OFA] preferred view). Note bilateral symmetry of the pelvis and femurs. The coxofemoral joints appear normal. **B,** Ventrodorsal distraction projection (PennHIP view) of the same dog. Bilateral coxofemoral laxity is evident.

the coxofemoral joints at their most congruent position. A distraction device is then placed between the femurs for the second radiograph (Fig. 21.33). When the femurs are pressed against the bars of the distractor, which act as a fulcrum, a lateral force is translated to the proximal femur, and any laxity leads to subluxation that can be visualized radiographically. The two views of the hips are compared, and any coxofemoral laxity is quantified by a unitless measure, the DI. The extended hip projection is also made so that secondary signs of hip dysplasia, such as degenerative joint disease, can be evaluated (Fig. 21.34).

The PennHIP method has inherent advantages over the extended hip method of evaluating the coxofemoral joints (Box 21.5). First, it quantifies joint laxity, which is generally accepted as the beginning of a chain of events that culminates in coxofemoral degenerative joint disease. Second, the examination can be performed on young dogs. The predictive value of the DI is constant after 6 months of age, thereby providing valuable information to breeders at an early age when selecting

Fig. 21.33 The distracted PennHIP view is achieved by holding a rubberized distraction device between the thighs, with the femurs at 90 degrees to the pelvis. The femurs are pressed gently against the distractor during radiography, thereby placing a lateral distraction force on the coxofemoral joints.

their stock. Third, the technique predicts a DI below which degenerative changes are unlikely to occur. Conversely, the DI and the subsequent development of degenerative joint disease appear to have a direct relation when the DI is greater than 0.3 (for German shepherd dogs) or 0.4 (for Labrador retrievers and rottweilers).

TRAUMA INVOLVING THE OSSEOUS COMPONENTS OF JOINTS

A fracture that communicates with a joint space is an articular fracture (Fig. 21.35). Articular fractures must be diagnosed accurately to ensure appropriate reduction and stabilization. Radiographic examinations should include two projections made at right angles to each other. Oblique views should be added, along with projections during flexion, extension, and stress, when needed. These additional projections are of most value when chip or avulsion fractures are suspected or when the osseous structures of interest are superimposed on other osseous structures.

Articular fractures occur frequently in immature animals because of the incidence of physeal and epiphyseal injury in these patients. Because the proximal femoral physis is intracapsular, all femoral capital physeal fractures are intraarticular fractures (Fig. 21.36). In other joints, physeal fractures that involve the joint are usually classified as Salter-Harris type III or IV fractures.[35]

SPRAINS AFFECTING JOINTS

Supporting soft tissue structures of joints appear as soft tissue opacities that silhouette each other and with adjacent soft tissues. Therefore they are not distinctly visualized radiographically. Radiographic features of severe sprains include (1) periarticular soft tissue swelling; (2) avulsion fractures at points of attachment of ligaments, tendons, and capsules to bone (entheses); (3) joint instability or subluxation; and (4) spatial derangement of the osseous components of a joint.

Sprains must be diagnosed promptly. In many instances, appropriate medical or surgical therapy ensures return to normal joint function after moderate to severe sprain injuries. Palpation and manipulation of a sprained joint is usually the best diagnostic tool. Radiographic examination adds information that is useful

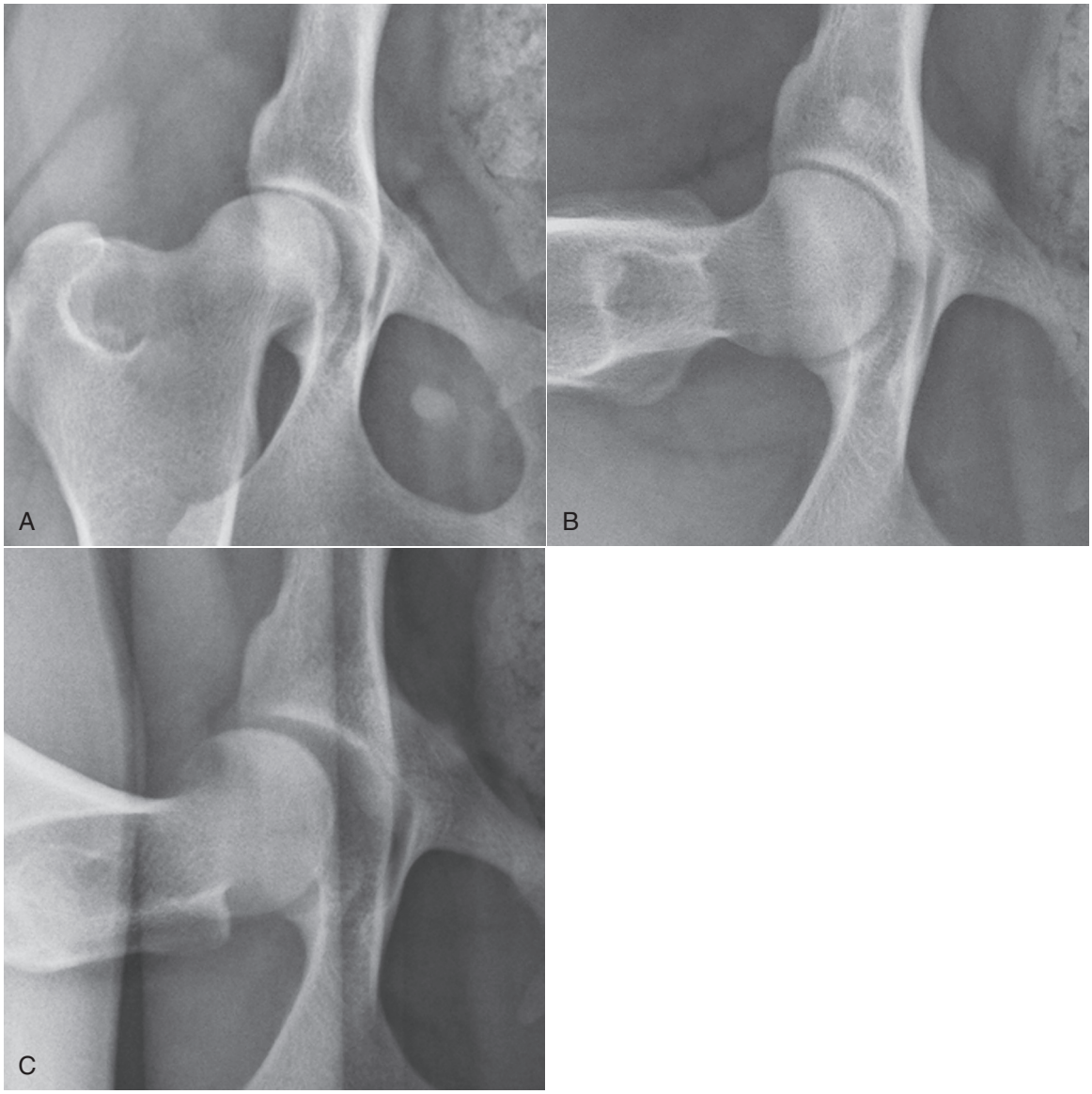

Fig. 21.34 Complete PennHIP study with the coxofemoral joints in the extended **(A)**, neutral compressed **(B)**, and distracted **(C)** projections. Note the amount of coxofemoral subluxation apparent in this dog with the distracted projection.

for treatment planning while documenting the presence and magnitude of the sprain and identifying avulsed osseous fragments. A useful technique for radiographic assessment of a sprained joint is stress radiography (Figs. 21.37 and 21.38). Stress radiography involves application of force to the joint to demonstrate displacement. The forces applied are the same stresses to which the joint would be subjected in normal daily activity and are defined as compressive, rotational, traction, shear, and wedge forces (Fig. 21.39).[36]

An example of a compressive stress is a radiograph of a joint during weight bearing. Ligamentous trauma, as in carpal hyperextension injuries, is readily detected by this technique. The cranial drawer sign seen in cranial cruciate ligament trauma is a practical example of a shearing stress. It is stress that is used routinely in clinical examination of the stifle. The same manipulative procedure may be applied to the stifle during radiography to capture the amount of cranial drawer in the image. Traction stress involves pulling the osseous components of the joint away from one another. One application of traction stress involves capital physeal fractures of the femoral head. When traction is applied to the femur in the extended ventrodorsal position, capital physeal fractures are more easily identified.

A technique using traction stress has been described for identifying medial scapulohumeral joint instability in small dogs. With the patient in lateral recumbency, nontraction and traction radiographs are made of the shoulder. A significant increase in joint space has been identified as a sign of medial shoulder instability. Traction and wedge stresses are useful for examining joints for small avulsion fractures and intraarticular joint mice. Unilateral trauma to collateral ligaments of the elbow and stifle may be disclosed with wedge stresses. Because stress radiography requires that personnel hold the patient during x-ray exposure, care must be taken to ensure that appropriate protective clothing is worn.

TENDONS, DESMOPATHIES

Injuries to tendons and ligaments are important causes of lameness in dogs and cats and must be distinguished

Fig. 21.35 **A,** A 3-year-old German shorthaired pointer with acute lameness of the left pelvic limb. There is a fracture through the lateral trochlear ridge of the talus *(open black arrow)*. **B,** Craniocaudal *(left)* and lateral *(right)* projections of a canine elbow with an intracondylar fracture extending through the medial humeral cortex. There is slight medial displacement of the fragment. Condylar involvement of the fracture is not apparent from the lateral projection. **C,** There are multiple patella fractures *(white arrows)*. Note the enthesophyte at the origin of gastrocnemius muscle *(black arrows)*. (**A,** Courtesy of University Veterinary Centre, Sydney, Australia. **B,** Courtesy of North Shore Veterinary Specialist Centre, Sydney, Australia.)

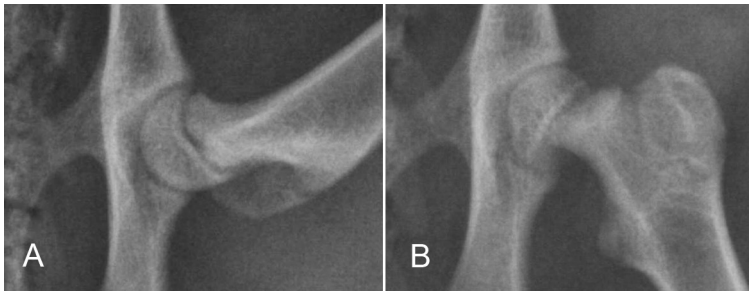

Fig. 21.36 The femoral capital physis appears wider than normal **(A),** which is confirmed in **B** by rotating the femur into a more extended position. This maneuver is useful to confirm this intraarticular fracture.

Box • 21.5

Comparison of Orthopedic Foundation for Animals and PennHIP Methods for Hip Dysplasia Radiography

Extended Ventrodorsal Projection

Advantages

Currently the most popular screening program internationally
- Does not require special training or accessory equipment
- Only one radiograph required
- Has amassed a large database of information about the coxofemoral phenotype
- Animals can be radiographed without personnel exposure

Disadvantages

Inaccurate in young animals; accuracy increases with age; optimal time to radiograph is 24 to 36 months
- An insensitive method of identifying coxofemoral joint laxity
- Requires rigid application to achieve beneficial results in breeding programs
- Technique of extending the femurs camouflages signs of joint laxity by spiral tensioning of the joint capsule

PennHIP Distraction Projection

Advantages

A valuable screening method for breeders before litters are placed in homes (as early as 16 weeks)
- An accurate method of predicting dysplastic changes in young animals from 6 months
- A sensitive method available for identifying joint laxity
- Generates a unitless index (distraction index [DI]) that can be used to predict whether degenerative joint disease will develop
- Has a greater heritability than the Orthopedic Foundation for Animals (OFA) method

Disadvantages

Requires special training to certify users
- Requires special equipment
- Multiple radiographic projections required
- Personnel exposure during radiographic exposure is difficult to avoid

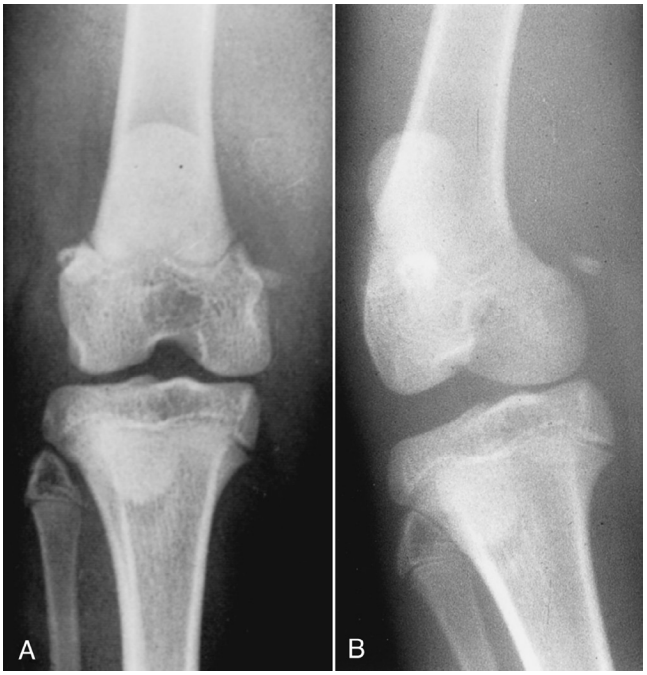

Fig. 21.37 An 8-month-old Burmese cat was lame in the left pelvic limb. A craniocaudal radiograph **(A)** was normal. In a stressed craniocaudal radiograph **(B),** widening of the lateral aspect of the joint space was apparent. The diagnosis is ruptured lateral collateral ligament.

from skeletal and articular causes of lameness. Many tendons and ligaments are intimately associated with joints, lying within them (cruciate ligaments), passing through them (bicipital tendon, long digital extensor tendon), or inserting adjacent to a joint (popliteus tendon). This section includes some of the common desmopathies that occur around joints.

Shoulder

Bicipital Tendon (Biceps Brachii)

Gross changes in dogs with bicipital tenosynovitis include synovial effusion, synovial hyperplasia of the bursa, chondromalacia of the intertubercular (bicipital) groove with osteophyte formation at its edges, and metastatic calcification of the biceps tendon. The two latter changes can be seen on survey radiographs of the shoulder (Fig. 21.40) when they occur in affected dogs. Occasionally discrete mineralized opacities (joint mice) may be seen superimposed on the tendon within the bicipital groove.[37] Sonography, CT and MRI are useful techniques for evaluating biceps and supraspinatus tendons. Biceps and supraspinatus tendons are closely associated, and enlargement of the supraspinatus tendon can impinge on the biceps tendon within the bicipital groove.

Ruptured Bicipital Tendon

Bicipital tendinopathy and bursitis may also be evaluated sonographically. In the longitudinal plane, the normal biceps tendon is characterized by an echogenic linear fiber pattern and can be followed from its origin at the supraglenoid tubercle of the scapula to its musculotendinous junction (Fig. 21.41). Sonography may reveal changes in the bicipital tendon or bursa in instances of bursitis and tendonitis (Fig. 21.42). The location of a rupture in the tendon may be identified sonographically. Sonography can also be used to identify the supraspinatus and infraspinatus tendons, the teres minor tendon, and the caudal aspect of the humeral head. Sonography assists in identification of synovial effusion and proliferation within the bicipital bursa, supraspinatus and bicipital tendonitis, dystrophic calcification, and osteochondrosis of the humeral head. Sonography can also be used to assist therapeutic joint or peritendinous injection. MRI has the advantage of superb soft tissue contrast resolution, which is valuable for assessing edema, hemorrhage, and inflammation within tendons and ligaments around joints.

The Carpus

Several important tendons pass close to the carpus or insert onto bones adjacent to it. Osteophytes arising and extending from the medial sulcus of the distal radius follow the path of the tendon of the abductor pollicis longus and are a response to synovitis where the tendon passes over the sulcus.

Fig. 21.38 **A,** A neutral lateral radiograph reveals slight incongruity of the distal intertarsal articulation *(arrow)*. **B,** Stress radiography revealed the extent and severity of dorsopalmar subluxation in the affected joint, while confirming stability in adjacent articulations.

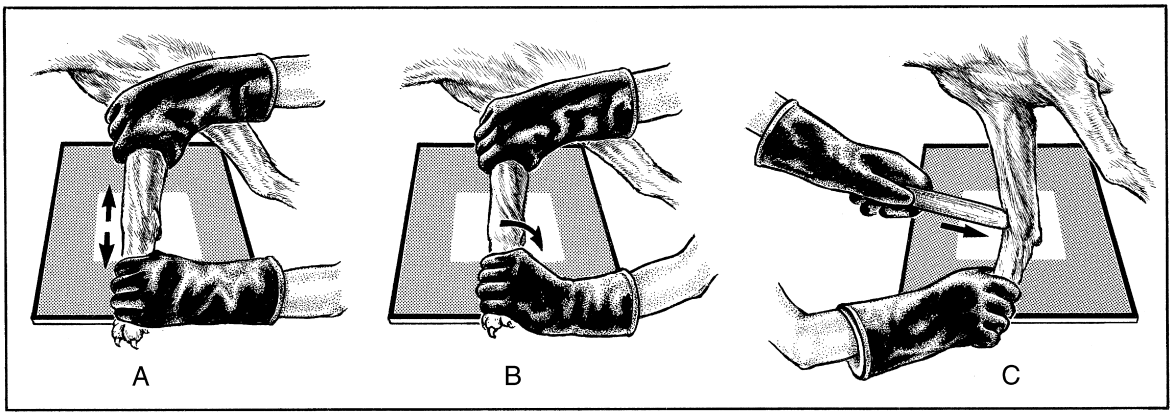

Fig. 21.39 Stress radiography of joints involves the application of traction **(A),** rotational **(B),** and wedge **(C)** forces to demonstrate subluxation that may not be evident on standard radiographic projections. (Modified from Farrow CS: Stress radiography: applications in small animal practice, *J Am Vet Med Assoc* 181:777, 1982.)

Osteophytosis has been associated with stenosis of the synovial sheath of the tendon.[38]

The extensor carpi radialis tendon inserts on the dorsal surface of the proximal end of metacarpals 2 and 3. Enthesopathy at the points of insertion can result in new bone formation that can be identified on lateral radiographs of the carpometacarpal region.

The flexor carpi ulnaris tendon inserts on the proximal surface of the accessory carpal bone, and the check ligaments of the accessory carpal bone originate from the distal surface. Again, an enthesopathy can be identified on the proximal and distal surfaces of the accessory carpal bone when an enthesopathy of these tendons and ligaments is present. The tendons and ligaments around the carpus can be assessed sonographically, as well as by MRI.

The Stifle

MRI can be used to assess structure and integrity of ligaments and tendons of the stifle. Changes in subchondral bone density and signal can be seen with CT and MRI (respectively) at the origin and insertion of the cranial cruciate ligament in patients with cranial cruciate strain. Indications for stifle sonography are limited but could include sonographic guided aspiration of synovial fluid or synovial masses.[39]

Tarsus

The common calcaneal tendon, or Achilles tendon, is composed mainly of the tendons of flexor digitorum superficialis and gastrocnemius muscles, with contribution of tendons from biceps femoris, semitendinosus, and gracilis muscles. It inserts onto the calcaneal tuberosity. Chronic desmopathies of the Achilles tendon cause soft tissue swelling, occasionally containing dystrophic calcification (Fig. 21.43). Sonography enables identification of partial and total ruptures of the deep and superficial structures comprising the Achilles tendon. A dynamic study can be used to assess the relationship between the Achilles tendon and its insertion onto the calcaneal tuberosity (Fig. 21.44). Tendinous trauma can be distinguished from muscle trauma.

HYPERVITAMINOSIS A

Excessive dietary vitamin A produces an ankylosing arthropathy and spondylopathy. Although both dogs and cats can be affected, the disorder is more likely to affect cats. The food mostly associated with hypervitaminosis A is bovine liver; and when fed as an exclusive diet, the clinical syndrome of vitamin A excess can be recognized after a few months. Affected cats

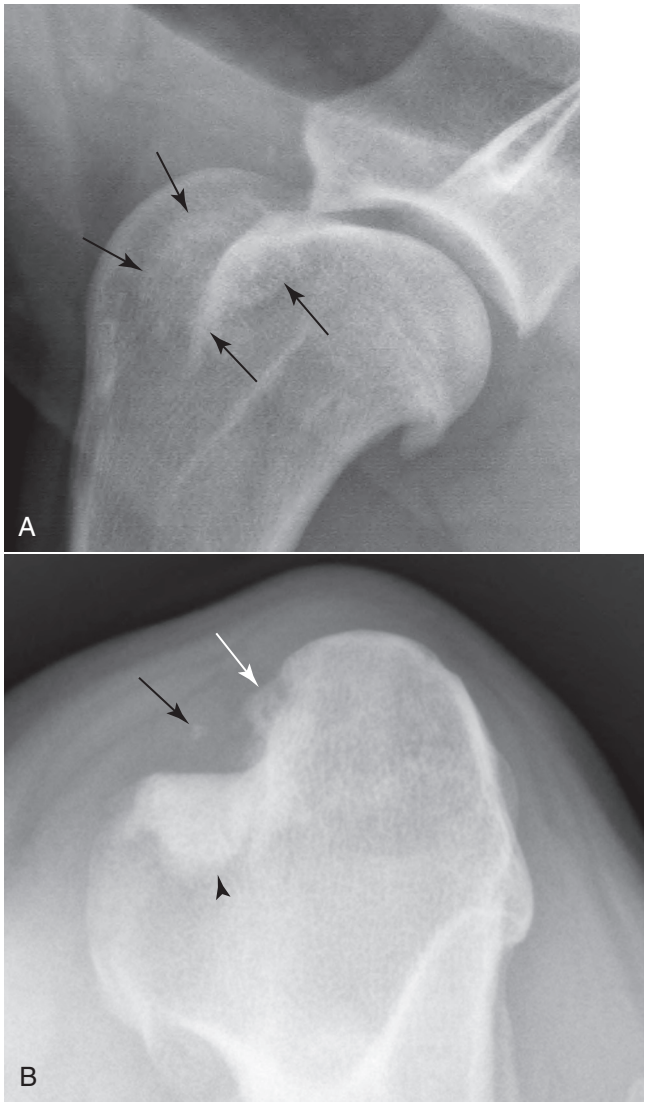

Fig. 21.40 Bicipital tendonitis. **A,** New bone proliferation superimposed on the bicipital groove *(black arrows)* and along the margin of the greater tubercle of the humerus seen in a dog with bicipital tendonitis. There is also a large osteophyte on the caudal aspect of the humeral head. **B,** A cranioproximal/craniodistal view of the proximal humerus. There are osteophytes in the bicipital groove *(white arrow)*, subchondral sclerosis of the groove *(black arrowhead)*, and a focus of mineralization in the biceps tendon *(black arrow)*.

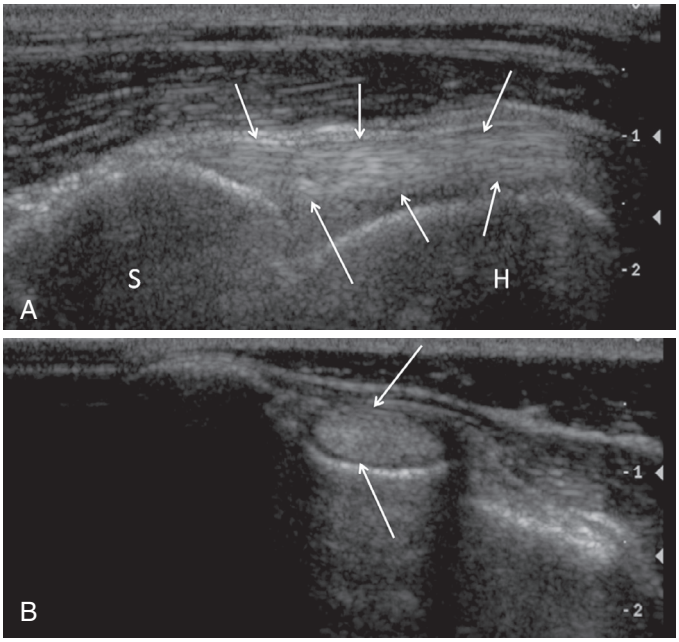

Fig. 21.41 Composite image showing longitudinal **(A)** and cross-sectional **(B)** images of the normal biceps tendon *(arrows)*. In a longitudinal plane **(A),** the tendon is characterized by a linear hyperechoic fiber pattern. The tendon arises from the supraglenoid tubercle of the scapula *(S)* and extends distally within the bicipital groove along the medial border of the humerus *(H)*. In cross section **(B),** the tendon is a uniformly hyperechoic oval structure surrounded by a thin hypoechoic rim representing slight fluid in the tendon sheath. (Reproduced with permission from Davies S, Allan G, Nicoll R: Joints—general. In Kirberger R, McEvoy F, Editors: *BSAVA manual of canine and feline musculoskeletal imaging,* ed 2, Gloucester, 2016, BSAVA.).

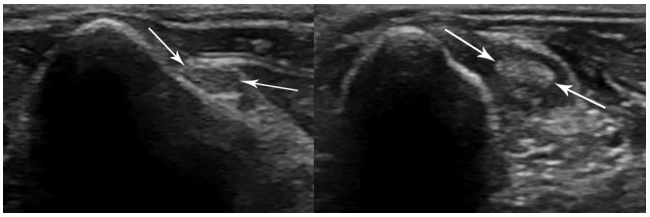

Fig. 21.42 Composite image showing a comparison of normal *(left)* and diseased *(right)* biceps tendons imaged in cross-section in the region of the bicipital groove. *Arrows* indicate the biceps tendon. The abnormal tendon is enlarged, has a slightly irregular outline, and is surrounded by hypoechoic fluid. (Courtesy of North Shore Veterinary Specialist Centre, Sydney, Australia.)

become obtunded, apprehensive, reluctant to jump, hypersensitive to neck palpation, and lame. The underlying connective tissue disorder causes vertebral ankylosis and an ankylosing degenerative joint disease of the forelimbs. Recognizable radiographic manifestations of hypervitaminosis A may be seen in as little as 10 weeks after introduction of a diet rich in vitamin A. Changes include ankylosing spondylopathy of the cervical and cranial thoracic vertebral column and periarticular enthesopathy and degenerative joint disease of shoulder and elbow joints (Figs. 21.45 and 21.46). In advanced disease, the additional bone becomes incorporated seamlessly with existing bone so that architecture of the original bones is remodeled completely. Other regions of the vertebral column and other joints of the appendicular skeleton may become involved, but the aforementioned bones and joints appear to be the primary site of bony changes in cats. The ankylosing changes are permanent. They do not resolve once a balanced diet is substituted, but some of the clinical signs of hypervitaminosis A resolve once the dietary imbalance is corrected.

MUCOPOLYSACCHARIDOSIS

Storage diseases that comprise MPS are characterized by tissue accumulation of glycosaminoglycans. Both dogs and cats can be affected by MPS, but the best-studied animal form is the feline form of mucopolysaccharidosis VI (MPS-VI). It causes polyarthropathies because of faulty cartilage formation, which is a result of dermatan sulfate accumulation in connective tissue because of deficiency of the lysosomal enzyme *N*-acetylgalactosamine-4-sulphatase. The morphologic appearance of affected cats ranges from normal to short-legged dwarfs with facial dysmorphism. Feline MPS-VI has two genotypes. The least affected phenotype ranges from being physically

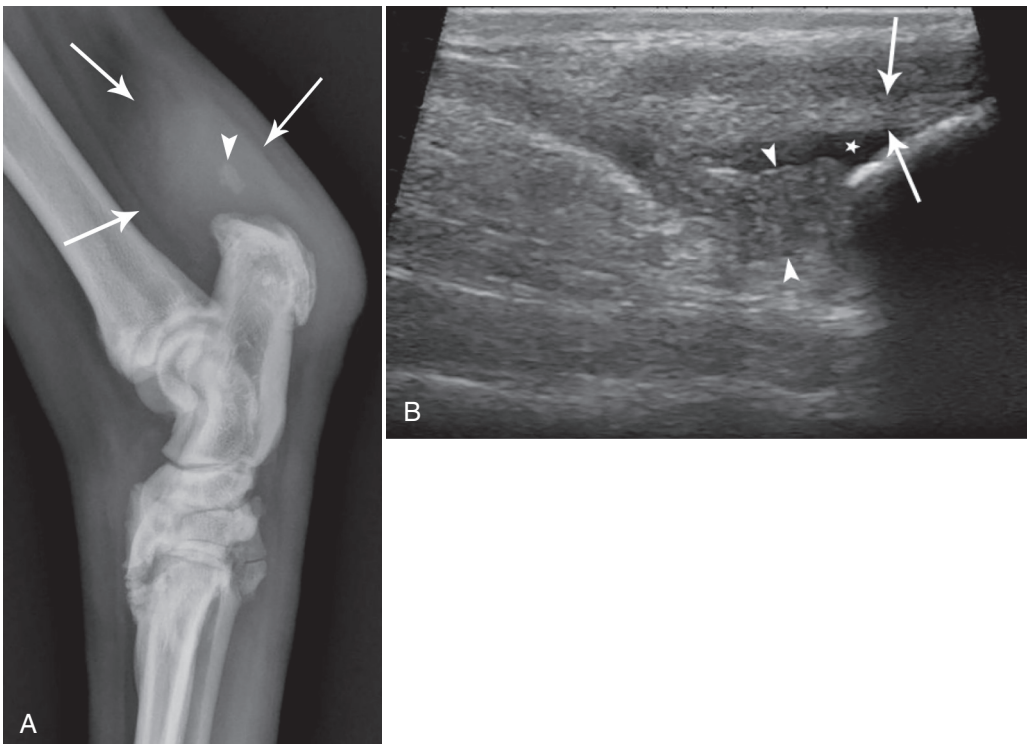

Fig. 21.43 Soft tissue swelling *(arrows)* and dystrophic calcification *(arrowhead)* in the region of the common calcaneal tendon in a dog **(A).** In the same patient **(B),** there is sonographic evidence of peritendinous fluid *(star)* and likely fibrinous material *(arrowheads)* in the caudal aspect of the tibiotarsal joint. The gastrocnemius tendon *(arrows)* inserts undisrupted onto the calcaneal tuberosity. (Courtesy of North Shore Veterinary Specialist Centre, Sydney, Australia.)

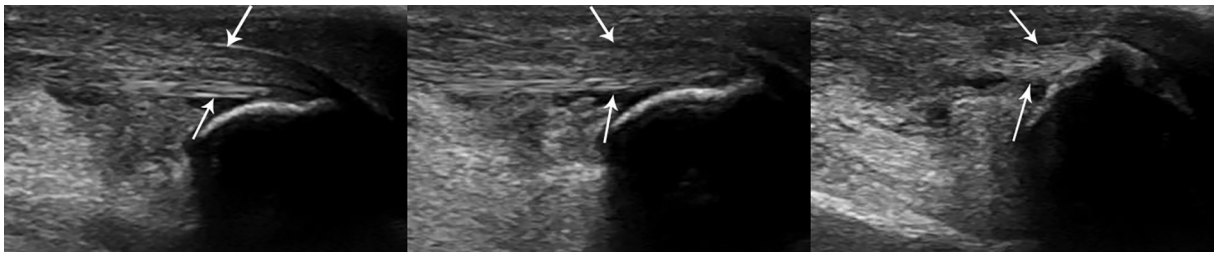

Fig. 21.44 Sonographic study in a dog presented with tarsal swelling after being hit by a car. Sequential images from left to right show progressive extension of the tibiotarsal joint. Attachment of the gastrocnemius tendon *(arrows)* to the calcaneal tuberosity is intact. (Courtesy of North Shore Veterinary Specialist Centre, Sydney, Australia.)

and clinically normal to having degenerative joint disease of the shoulder and stifle joints. The classic form produces phenotypic features of dwarfism and facial dysmorphia. These cats tend to have lameness and develop hind limb paresis. Radiographic abnormalities reflect epiphyseal dysplasia and range from degenerative joint disease in the shoulder and stifle to gross malformation of the appendicular and axial skeleton (Figs. 21.47 and 21.48). Severely affected animals are osteopenic. Subchondral bone of articular surfaces is distorted, and periarticular soft tissue mineralization is common. A high level of lysosomal storage in chondrocytes adversely affects mineralization of matrix during enchondral ossification, resulting in epiphyseal dysplasia and distortion of epiphyses of the appendicular skeleton. Vertebral malformation is a recognizable feature of feline MPS-VI. Vertebral bodies are short and square, the pedicles elongated, and articular processes malformed. Epiphyseal dysplasia causes distortion of the epiphyses of vertebral bodies. New bone formation around articular processes and ankylosing spondylopathy are common.

SCOTTISH FOLD CHONDRO-OSSEOUS DYSPLASIA

Scottish fold chondro-osseous dysplasia (SFCOD) is an inherited autosomal dominant trait that causes defective cartilage maturation.[33] Although folding of the ear cartilage is a defining visible feature of SFCOD, the cascade of changes caused by faulty cartilage maturation affecting the skeleton are seen in both homozygotes and heterozygotes. In extreme forms, the polyarthropathy caused by SFCOD can be crippling, and affected animals can be disinclined to ambulate and unable to jump. Defective cartilage formation manifests skeletal changes that affect joints and entheses. Joints of the distal limbs are affected most spectacularly, but some long bones (such as, the metacarpi,

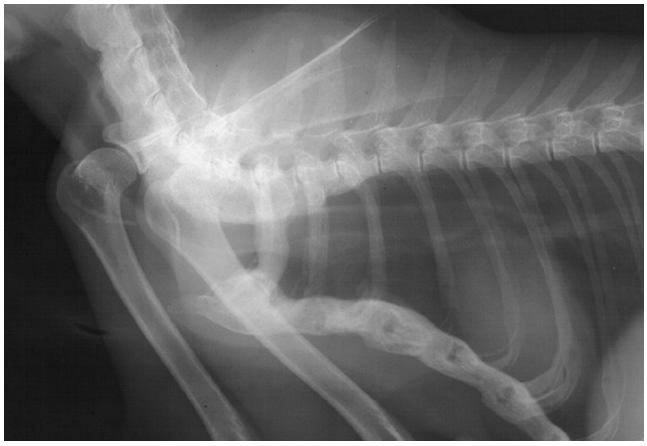

Fig. 21.45 Ankylosing spondylopathy of the cervical and cranial thoracic vertebrae and the sternum of a cat with hypervitaminosis A. (Reprinted from Allan GS: Radiographic features of feline joint diseases, *Vet Clin North Am Small Anim Pract* 30:281, 2000. Courtesy University of Queensland, Brisbane, Australia.)

metatarsi, and phalanges) may also develop abnormally (Fig. 21.49). Large enthesophytes can form around joints at points of tendinous origin or insertion (entheses). An ankylosing arthropathy frequently results in fusion of the carpi and tarsi (Fig. 21.50) and their articulations with the metacarpi and metatarsi. Malformed bones in the manus and pes may not grow to a normal length, and these bones may appear shorter and fatter than normal. Vertebral malformation can also occur in the tail, where the caudal vertebrae may be short and wide. Spondylopathy of the caudal vertebrae may combine to produce a tail that is short and relatively inflexible.[41]

HEMARTHROSIS

Intraarticular hemorrhage may occur in dogs with coagulopathies or after joint trauma.[42] Coagulopathies in the dog that may cause hemarthrosis include hemophilia A and B; von Willebrand disease; deficiencies in factors VII, X, and XI; and liver disease. Isolated, infrequent episodes of intraarticular bleeding do not significantly alter joint cartilage integrity. Repeated hemorrhage

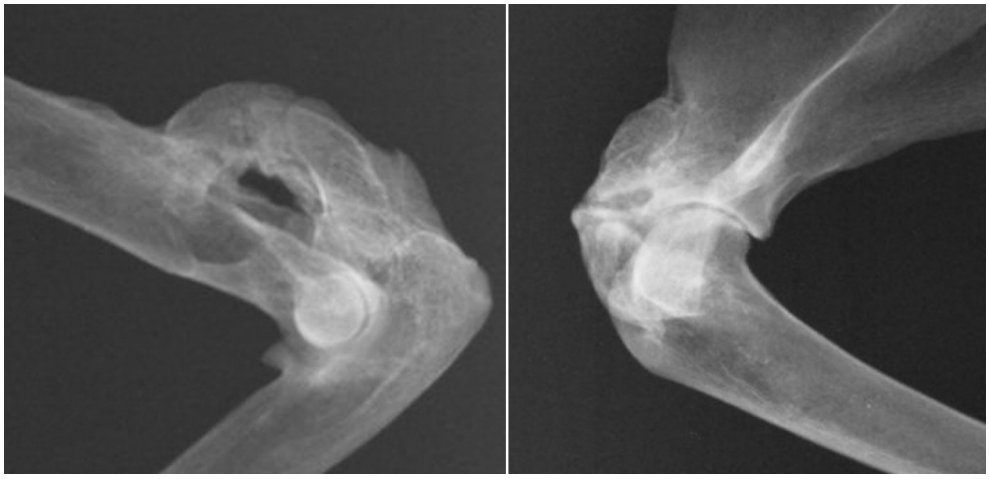

Fig. 21.46 Radiographs of the elbows and a shoulder from the skeleton of a cat that was euthanized because of ankylosing arthropathy caused by hypervitaminosis A.

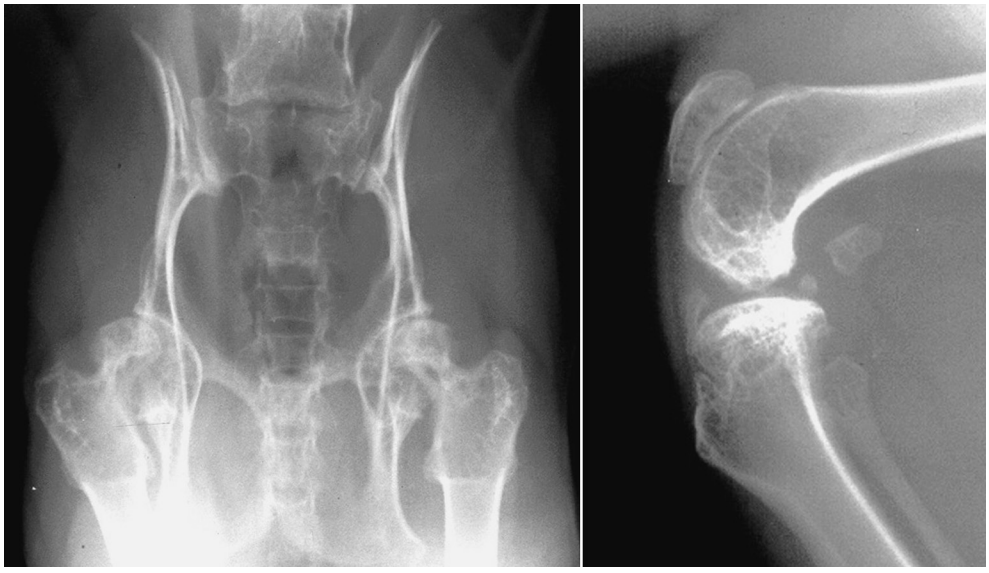

Fig. 21.47 Malformation of the coxofemoral joints, pelvis, and stifle caused by mucopolysaccharidosis VI (MPS-VI) in a cat. (Courtesy of Dr. A. C. Crawley, Adelaide, South Australia. Reprinted from Allan GS: Radiographic features of feline joint diseases, *Vet Clin North Am Small Anim Pract* 30:281, 2000.)

Fig. 21.48 Cervical vertebral malformation caused by mucopolysaccharidosis (MPS) in a cat. (Courtesy of Vet HQ, Sydney, Australia)

Fig. 21.49 Carpometacarpal ankylosis and metacarpal and phalangeal malformation in a Scottish fold cat. (Courtesy of Jimmy Lattimer.)

Fig. 21.50 Tarsal and tarsometatarsal ankylosis and metatarsal malformation in a Scottish fold cat with Scottish fold chondro-osseous dysplasia (SFCOD). (Courtesy of Jimmy Lattimer.)

may lead to severe damage to joint cartilage and subchondral bone. Affected animals have severe non–weight-bearing lameness of affected limbs, and affected joints are swollen and painful. Radiographically, in acute hemarthrosis there is soft tissue swelling of the joint, which may be extensive.[42] As a consequence of chronic intraarticular hemorrhage, joint cartilage may be eroded and thin and subchondral bone can appear irregular. Repeated injection of whole blood into stifle joints results in remodeling of bones adjacent to the joint. In advanced hemarthrosis, signs similar to degenerative joint disease may be present.

SEPTIC ARTHRITIS

Septic arthritis is diagnosed infrequently in small animals, with the incidence being lower than that of immune-mediated joint disease. Septic arthritis is difficult to diagnose radiographically. Initial radiographic changes are usually limited to joint effusion and periarticular swelling. Ideally, the arthritis should be diagnosed and treated successfully before radiographic changes become apparent.[43] Polyarticular septic arthritis may occur as a result of bacteremia associated with an isolated focus of infection (endocarditis, discospondylitis, or omphalophlebitis) or in conjunction with a systemic disease (as in *Mycoplasma* arthritis, canine leishmaniasis, or feline caliciviral lameness).[44] Polyarticular septic arthritis must be differentiated from immune-mediated joint disease. The former is more likely to affect the larger, more proximal joints of the appendicular skeleton, whereas the latter more commonly affects the joints nearer the distal extremities (Box 21.6). Monoarticular septic arthritis most likely results from extension of focal osteomyelitis into an adjacent joint, direct joint trauma, or foreign body penetration (grass seed awns), or it may occur after joint surgery or intraarticular therapy. Hematogenous dissemination of infection to joints is more common in young animals. Septic arthritis as a complication of surgery, particularly addressing cranial cruciate insufficiency, is more common in older animals.

As already noted, the earliest radiographic changes of septic arthritis are synovial effusion and increased synovial mass, which represent an inflammatory response of the synovium. Soft tissue swelling is usually demarcated by the distended joint capsule. Joint capsule distention is identified more easily in carpal, tarsal, and stifle joints. A useful landmark in the stifle is the infrapatellar fat pad. When the fat pad is compressed cranially, it becomes smaller and unclear, indicating synovial effusion is present. In untreated septic arthritis, joint cartilage destruction follows synovial effusion and is followed by subchondral and perichondral bone destruction (Figs. 21.51 and 21.52; Box 21.7).

Septic arthritis is being identified increasingly in joints that have chronic degenerative joint disease. Initial radiographs are characterized by degenerative joint disease, often leading to inappropriate therapy for the infection. Radiographs made 2 to 4 weeks later reveal more aggressive signs of periosteal new bone formation and intraarticular bone destruction. Septic arthritis should be suspected when acute lameness and joint pain are identified in individual animals whose degenerative joint disease has been controlled previously.

Diagnosis of septic arthritis is based on cytologic assessment of synovial fluid and microbiologic examination of synovial fluid and/or synovium and joint capsule. Radiographic assessment

alone has low specificity for septic arthritis, but survey radiographs are useful to rule out other conditions, as well as to follow the progress of a joint infection once a diagnosis of septic arthritis is confirmed.

Septic Arthritis in Cats

In cats, hematogenously disseminated septic arthritis may be caused by a variety of microorganisms, which include *Mycoplasma gateae, Mycoplasma felis,* bacterial L-form infection (*Pasteurella* spp.), calicivirus (transient arthritis in kittens),

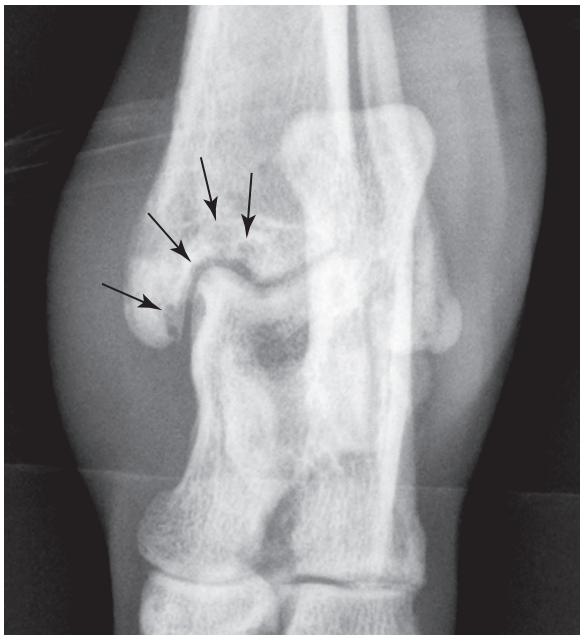

Fig. 21.51 A 1.5-year-old canine mix with lameness and tarsal swelling for 2 weeks. There are focal subchondral lucencies in the distomedial aspect of the tibia *(black arrows)*. The swelling is also obvious. Cryptococcus was isolated from synovial fluid.

Box • 21.6

Polyarthropathies Affecting the Appendicular Skeleton of Dogs and Cats

- Immune-mediated joint diseases
  - Rheumatoid arthritis
  - Systemic lupus erythematosus (SLE)
  - Feline periosteal proliferative polyarthritis
  - Feline nonerosive immune-mediated polyarthropathy
- Septic arthritis
  - Hematogenous septic arthritis
  - Bacterial or fungal septic arthritis
- Inflammatory arthritides
  - Leishmaniasis
  - Rocky Mountain spotted fever
  - Rickettsia rickettsii
  - Lyme disease
  - *Borrelia burgdorferi*
  - Mycoplasma arthritis
  - Chinese shar-pei fever syndrome
  - Feline calicivirus, coronavirus
  - Greyhound polyarthritis
- Hemarthrosis
  - Chronic, recurrent, caused by blood dyscrasias
- Hypervitaminosis A
- Primary degenerative joint disease/osteoarthrosis
- Disseminated idiopathic skeletal hyperostosis syndrome
- Familial or genetic skeletal dysplasias
  - Scottish fold osteochondrodysplasia
  - Feline mucopolysaccharidosis (MPS)
  - Canine hip dysplasia
  - Canine elbow dysplasia
  - Osteochondrosis
- Drug-induced and vaccine-mediated polyarthritis
- Feline osteochondromatosis

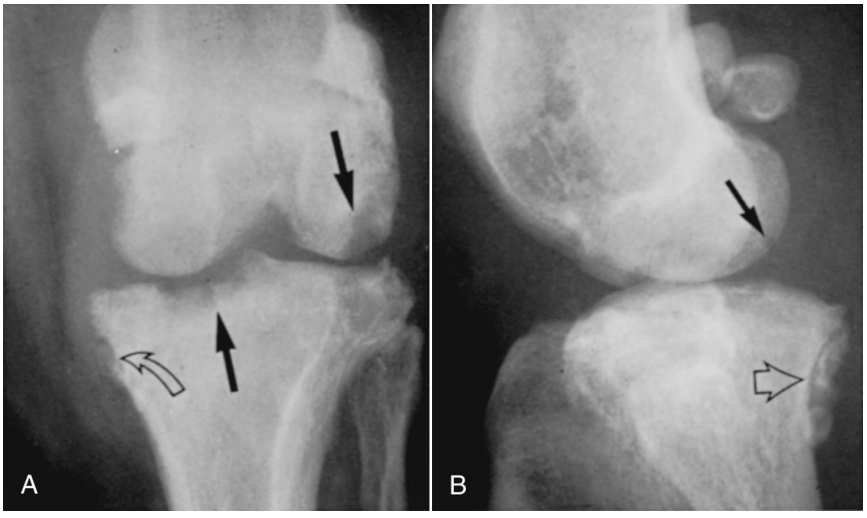

Fig. 21.52 An 8-year-old male Australian cattle dog had stifle swelling and pain that persisted after repair of a ruptured cranial cruciate ligament. **A** and **B,** Subchondral bone erosion involves the medial condyle of the tibia and the femoral condyles *(solid black arrows)*. Periarticular new bone formation is also evident *(open black arrow)*. Note the concurrent medial patellar luxation. *Staphylococcus aureus* was isolated from the synovial fluid.

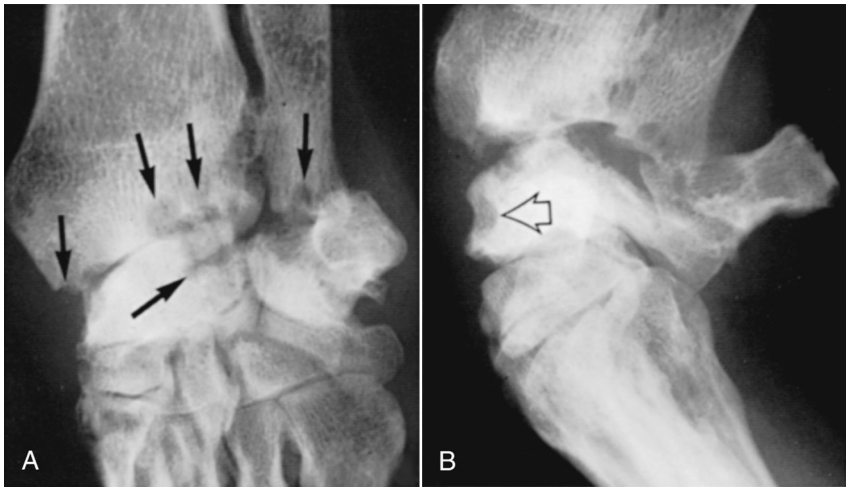

Fig. 21.53 An 8-year-old male (neutered) Corgi crossbreed with rheumatoid arthritis. **A,** Dorsolateral-palmaromedial projection. There is extensive subchondral erosion of the styloid process of the ulna and the articular surfaces of the distal radius and radial carpal bone *(black arrows)*. **B,** Lateral projection during flexion. In addition to the changes seen in **A,** note the erosion of the non–weight-bearing dorsal surface of the radial carpal bone *(open black arrow)*. (Courtesy of University Veterinary Centre, Sydney, Australia.)

Box • 21.7

Progression of Radiographic Signs of Infectious Arthritis

- Increased synovial mass indicating synovial effusion and widened radiolucent joint space
- Diminished radiolucent joint space indicating destruction of articular cartilage
- Loss of the smooth surface of the subchondral bone plate; an early sign of infectious penetration of subchondral bone
- Osteolucent signs of destruction of subchondral and perichondral bone usually highlighted by a peripheral border of increased osseous opacity
- In advanced infectious arthritis, weight-bearing surfaces may collapse, causing distortion of joint architecture

coronavirus (feline infectious peritonitis), and fungi (cryptococcosis, histoplasmosis). Hematogenously disseminated septic arthritis initially causes a nonerosive polyarthropathy characterized by lameness, synovial effusion, and synovial thickening. Affected cats may be systemically ill. Viremic polyarthropathies tend to be transient, whereas bacterial arthritis can have a protracted course. Direct injection of bacteria from bite wounds can result in mixed infections of microorganisms, which may include anaerobic bacteria.

Septic arthritis from penetrating bite wounds causes lameness that is usually restricted to one joint. Synovial effusion and periarticular soft tissue thickening precede secondary changes (such as, subchondral bone erosion) by weeks or months. CT can facilitate early detection of bone erosions and demonstrate synovitis. Joint infections that extend through the synovium and joint capsule into extracapsular tissue stimulate periosteal new bone formation on bone surfaces adjacent to the joint. Septic arthritis can lead to osteomyelitis in bones on either side of an affected joint.

IMMUNE-MEDIATED ARTHROPATHIES

Rheumatoid Arthritis

Rheumatoid arthritis is a severe, progressive, erosive polyarthritis that has been reported in dogs,[45] and a similar condition has been reported in cats.[46] Radiographic changes usually occur in joints of the distal extremities. The stifle and elbow are affected occasionally. Synovial effusion occurs initially. Radiographs made early are characterized by nonspecific periarticular soft tissue swelling. The joint capsule may be distended. The first radiographic signs of bone involvement may be detected several weeks after the onset of clinical signs. Initial changes are mild, but the radiographic abnormalities become more obvious as the disease advances.

The progression of radiographic changes includes (1) subchondral bone destruction and cyst formation (Fig. 21.53); (2) joint space narrowing; (3) progressive decreased opacity of epiphyses adjacent to affected joints; (4) destruction of subchondral and perichondral bone; (5) mushrooming of the ends of the metacarpi and metatarsi, which occurs in advanced arthritis and represents collapse of subchondral bone; and (6) varying degrees of joint subluxation and luxation (Fig. 21.54). Other changes more characteristic of degenerative joint disease (osteophytes/enthesophytes, subchondral sclerosis, and calcified periarticular tissues) may also be present.[45]

Systemic Lupus Erythematosus

Systemic lupus erythematosus (SLE) is a multisystemic disease that affects dogs of all breeds, as well as cats. It has a variety of clinical manifestations, including polyarthritis, anemia, nephropathy, skin disease, pericarditis, myocarditis, and lymphadenopathy.[47] Diagnosis of SLE is complicated and is made on the basis of the concurrence of clinical manifestations and serologic evidence. In one study, 121 dogs with a diagnosis of SLE were reviewed, and joint disease was reported to be the most frequent clinical sign (69%), followed by hematologic (53%), renal (50%), cutaneous (33%), and intrathoracic (17%) manifestations. The arthropathy that occurs in canine SLE is usually nonerosive and effusive. Polyarthritis is typical, but monoarticular arthritis has been reported. Affected joints may be swollen, painful, and warm. The joints most commonly affected are the carpus, tarsus, metatarsus, stifle, and elbow.

Fig. 21.54 Dorsopalmar radiographs of the left **(A)** and right **(B)** manus of a dog with immune-mediated arthropathy. There is subluxation of the left antebrachiocarpal joint and the right carpometacarpal joint. There is also subluxation of distal interphalangeal joint in each manus. Numerous subchondral lytic erosive lesions are present *(white arrows)*.

Radiographic signs are usually absent or are minimal. In chronic SLE, the joint space of affected joints may be narrowed, and the joint capsule is distended. A mild periosteal response has been reported at the junction of joint capsule and bone.

Feline Noninfectious Polyarthritis

Feline noninfectious polyarthritis is a disease of male cats aged 1 to 5 years.[46,48] The polyarthritis can be erosive or nonerosive.[49] There are two types of erosive polyarthritis: (1) the periosteal proliferative form and (2) the erosive form. The erosive form is commonly referred to as *feline rheumatoid arthritis*. A group of nonerosive, effusive polyarthropathies thought to be immune mediated also occur in cats and are associated with a variety of conditions.

Periosteal Proliferative Form

Affected cats have fever, malaise, and stiffness, followed by periarticular soft tissue swelling and regional lymphadenopathy. Radiographic changes may be identified in affected joints after a few weeks. Commonly affected joints are the carpi and tarsi. The stifle, elbow, shoulder, and hip joints are affected to a lesser extent. During the first month, periarticular soft tissue swelling is the predominant sign. Swelling may be either intracapsular or extracapsular. One to 3 months after the onset of clinical signs, periosteal new bone production may be identified at site of joint capsule attachment. During this phase, bone adjacent to affected joints may have decreased opacity and a coarse trabecular pattern. Perichondral new bone formation is pronounced 2 to 3 months after onset of the disease. Extensive enthesopathy may bridge smaller joint spaces. More severe radiographic manifestations include perichondral bone erosion and formation of subchondral cysts. Narrowing of affected joint spaces may occur late.[46] Radiographic signs of the periosteal proliferative form of feline chronic progressive polyarthritis include periarticular soft tissue swelling, periosteal new bone formation, perichondral enthesophyte production, perichondral and subchondral erosion, subchondral cysts, osteopenia of bone adjacent to affected joints, and narrowed joint spaces (Fig. 21.55).

Fig. 21.55 The carpus of a young cat with feline chronic progressive polyarthritis. (Courtesy of University Veterinary Centre, Sydney, Australia. Reprinted from Allan GS: Radiographic features of feline joint diseases, *Vet Clin North Am Small Anim Pract* 30:281, 2000.)

Erosive Form

A second, more erosive form of feline noninfectious polyarthritis has been described; it resembles human rheumatoid arthritis and is seen in older cats.[46] This form is characterized radiographically by severe subchondral bone erosion, perichondral bone erosion, and subchondral cyst formation. Perichondral enthesophyte formation, bone destruction at points of ligamentous insertion to bone, and subluxation of small joints of the extremities also occur. A diagnosis of feline rheumatoid arthritis requires a positive rheumatoid factor test, characteristic histologic changes seen on a synovial biopsy, or both. Both test results are negative in cats with feline proliferative polyarthritis.[49]

Feline Nonerosive Polyarthritis

Two categories of nonerosive polyarthritis have been described in cats.[49] They are feline SLE and idiopathic polyarthritis. Idiopathic polyarthritis has four subtypes: (1) uncomplicated polyarthritis; (2) reactive polyarthritis, associated with a disease process elsewhere in the body; (3) enteropathic polyarthritis, associated with gastrointestinal disease; and (4) malignant-related idiopathic polyarthritis, associated with myeloproliferative disease. Radiography is used to distinguish between erosive and nonerosive forms of feline polyarthritis. The latter group is identified as having periarticular soft tissue swelling, joint capsule distention, and synovial fluid accumulation.

Hypertrophic Osteopathy

Hypertrophic osteopathy is a generalized osteoproductive disorder of the periosteum that affects the long and short tubular bones of the extremities. It is usually caused by a thoracic mass or cardiopulmonary disease. Abdominal masses, particularly those of urinary origin, have also been known to cause hypertrophic osteodystrophy. Nonneoplastic causes of hypertrophic osteopathy include inflammatory lung disease (e.g., blastomycosis), intrathoracic foreign bodies, *Dirofilaria*

immitis infestation, and spirocercosis. The pathogenesis of hypertrophic osteopathy is understood incompletely. New bone formation typically commences on the distal end of both short and long tubular bones and progresses proximally. Periosteal new bone formation results in cortical thickening. The periosteal surface appears nodular or spiculated when visualized radiographically (Figs. 21.56 and 21.57).

THE SYNOVIUM

Villonodular Synovitis

Villonodular synovitis is an intracapsular joint disorder characterized by nodular synovial hyperplasia, which is thought to represent a response to trauma. Experimentally, villonodular synovitis has been reproduced in dogs by repeated intraarticular injections of whole blood. Villonodular synovitis is an established, although uncommon, disorder of humans and has also been reported in horses and dogs.[50,51] In dogs, the condition has been identified in the carpus, coxofemoral joint, and stifle. Radiographic signs of villonodular synovitis may be nonspecific but include articular soft tissue swelling alone or with erosion of cortical bone at the chondrosynovial junction (Fig. 21.58). These cortical erosions may appear cyst like, with slightly opaque borders. In severe proximal femoral villonodular synovitis in humans, the femoral neck has been described as looking like an apple core. The articular cartilage and subchondral bone are not involved. Differential diagnoses for perichondral erosive lesions, characteristic of villonodular synovitis, include synovial osteochondromatosis, rheumatoid arthritis, and joint neoplasia.

Synovial Osteochondromas

Synovial osteochondromas are islands of cartilage produced by the synovial membrane. Foci of cartilage become pedunculated and may become separated to form loose bodies within the joint. Reports of synovial osteochondromatosis in cats suggest that Burmese cats are overrepresented. The radiographic appearance of mineralized synovial osteochondromas varies. These lesions are usually well-defined, rounded, often multiple intraarticular nodules of calcific opacity (Fig. 21.59). Synovial osteochondromas may also arise from extraarticular foci of synovial tissue (Fig. 21.60).

Synovial osteochondromas have been reported in the dog and the cat.[52,53] Their cause is unknown, but the theory of synovial metaplasia is generally accepted. These lesions have been reported to cause severe lameness in some dogs. Surgical removal of synovial osteochondromas relieves clinical signs of joint pain and lameness.[52] Other conditions in cats in which intraarticular and periarticular mineralization may be confused with synovial osteochondromatosis are mild forms of MPS-VI and hypervitaminosis A.[40]

Joint Neoplasia

Synovial sarcoma arises from primitive mesenchymal precursor cells of the synovial membrane of joints and bursae.[54] These

Fig. 21.56 Radiograph of the manus of a dog with hypertrophic osteopathy. There is irregular periosteal reaction *(arrows)* that is most pronounced on the lateral aspect of the fifth metacarpal bone and on the medial aspect of the distal radius. There is less pronounced periosteal reaction on the medial aspect of the manus.

Fig. 21.57 Lateral radiographs of the crus **(A)** and antebrachium **(B)** of a dog with hypertrophic osteopathy that is more advanced than in Fig. 21.56. The abnormal periosteum has progressed to involve the more proximal aspect of the long and short tubular bones.

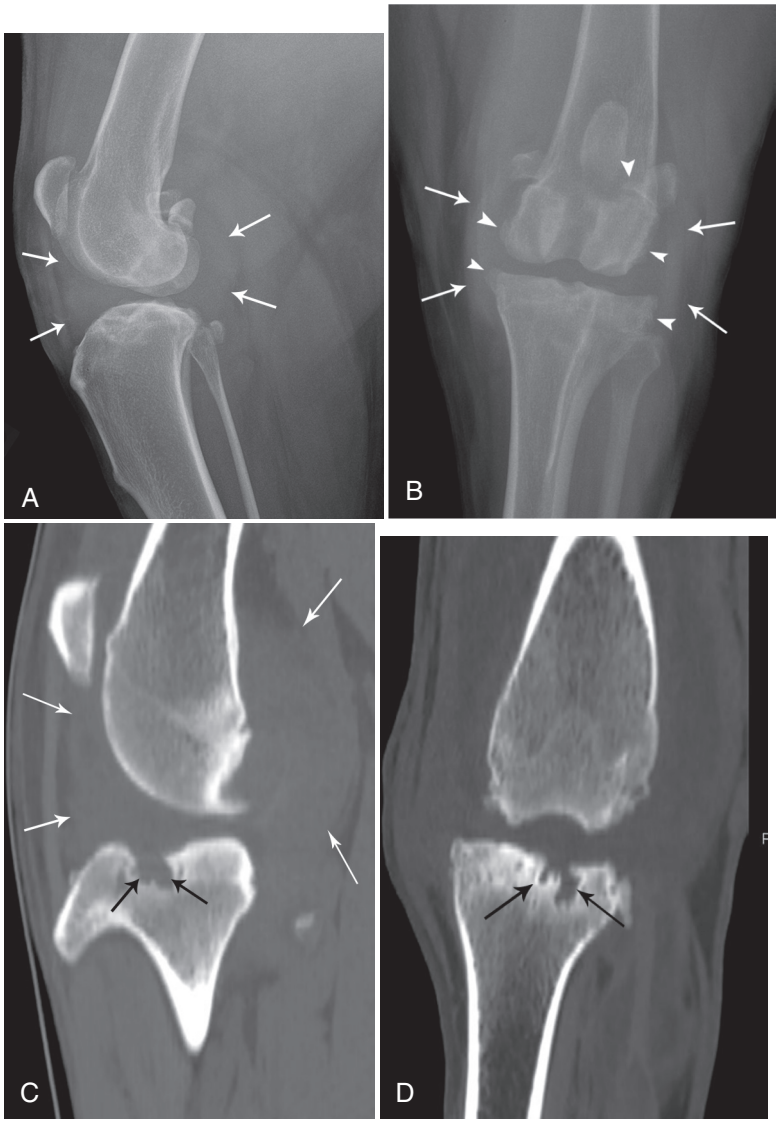

Fig. 21.58 Lateral **(A)** and craniocaudal **(B)** radiographs of the stifle of a dog with a histopathologic diagnosis of villonodular synovitis. There is marked intracapsular soft tissue swelling *(white arrows)* and osteophytes are present on periarticular surfaces *(arrowheads)*. Loss of bone *(black arrows)* is detected with computed tomography (CT) in the cranial intercondylar region **(C** and **D).** (Courtesy of Animal Orthopaedic Specialists, Sydney, Australia.)

Fig. 21.59 A 5-year-old Burmese cat had bilateral stifle enlargement. Extensive lobular mineralization within the stifle joint was evident radiographically. Histologic diagnosis was synovial osteochondroma. (Courtesy of Perth Veterinary Specialists, Perth, Australia.)

Fig. 21.60 A 6-year-old male (neutered) Burmese cat had progressive lameness of the right forelimb for 6 weeks. Radiographically, a large, well-defined, ossified mass was visible on the craniomedial aspect of the right elbow. Histologic diagnosis was extraarticular synovial osteochondroma.

Fig. 21.61 **A,** A cystic lesion was identified in the distal end of the left ulna *(white arrows)* 6 weeks after the onset of soft tissue swelling around the antebrachiocarpal joint. **B,** The lesion progressed over the succeeding 12 months, by which time a multiloculated cyst like change was present in the distal radius, ulna, and the proximal row of carpal bones. Histologic diagnosis was synovial cell carcinoma. (Courtesy of Dr. P. Young, All Pets Veterinary Hospital, Albury, Australia.)

tumors are uncommon in the dog and rare in the cat.[55] They occur most frequently in middle-aged, medium-sized to large dogs. The most commonly affected joints are the stifle and elbow. Synovial sarcomas grow slowly and are first noticeable as a homogeneous soft tissue mass that involves or is near a joint. Portions of the tumor may be calcified, with mineral deposits appearing as hazy and punctate or as linear streaks.

Initial bone involvement usually appears as a spiculated periosteal response followed by ragged erosion of cortical bone adjacent to the tumor. Occasionally the neoplasm initially appears relatively nonaggressive, mimicking a simple cyst, only to change later into a more extensive and destructive disease (Fig. 21.61). Destruction of cancellous bone may be extensive and most commonly occurs on both sides of the joint. The tumor is locally invasive with a capacity to metastasize.[56] Distant metastasis, particularly to the lungs, occurs in as many as half of reported patients.[54]

Many neoplasms mimic the radiographic appearance of synovial sarcomas (Fig. 21.62). In a study of joint neoplasms, synovial sarcomas were represented in only 27% of patients.[57] Other neoplasms with a radiographic appearance similar to that of synovial sarcomas included fibrosarcoma, rhabdomyosarcoma, fibromyxosarcoma, malignant fibrous histiocytoma, liposarcoma, and undifferentiated sarcoma. Primary bone tumors can occur in close proximity to a joint and can extend to involve destruction of subchondral bone (Fig. 21.63).

Histologic evaluation of the lesion is mandatory to establish its origin.

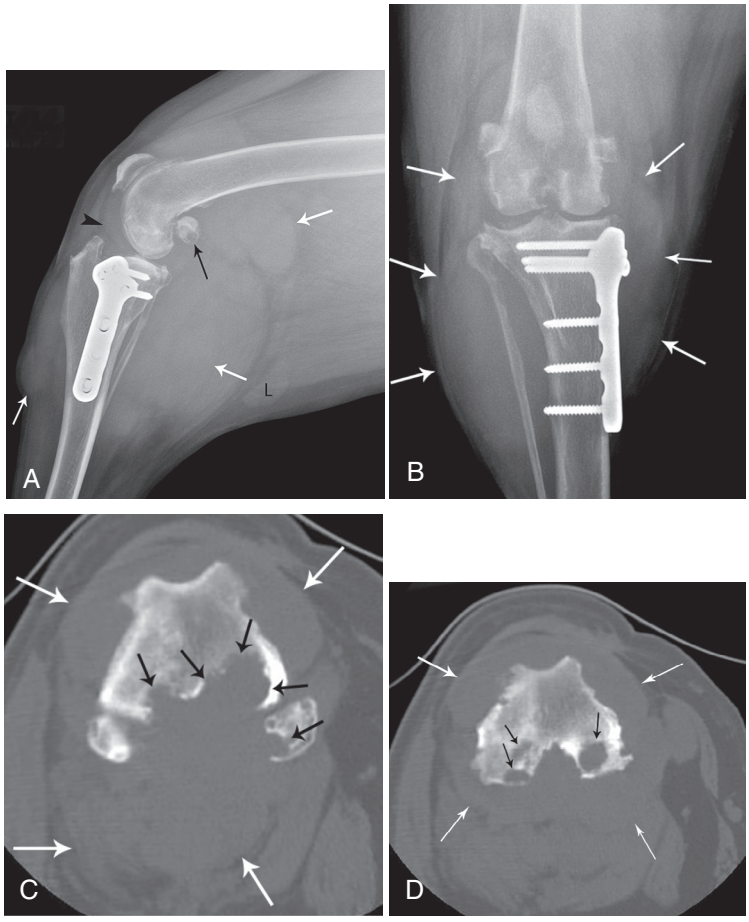

Fig. 21.62 Lateral **(A)** and craniocaudal **(B)** radiographs of the stifle with extensive intracapsular and extracapsular soft tissue swelling. A tibial plateau leveling osteotomy (TPLO) had been performed previously; note the bone plate on the medial aspect of the tibia. *White arrows* indicate extent of soft tissue swelling. *Black arrowhead* indicates effacement of the infrapatellar fat pad as a sign of intraarticular soft tissue swelling. The distal femur and supracondylar areas have a mottled appearance and lucent foci are present in the fabellae *(black arrow)*. The popliteal lymph node is within normal limits for size (L). Axial computed tomography (CT) images **(C** and **D)** show the extent of osteolysis involving the femoral condyles and fabella medial *(black arrows)*. Final diagnosis was histiocytic sarcoma. There is no presumed association with the prior TPLO. (Courtesy of Animal Orthopaedic Specialists, Sydney, Australia.)

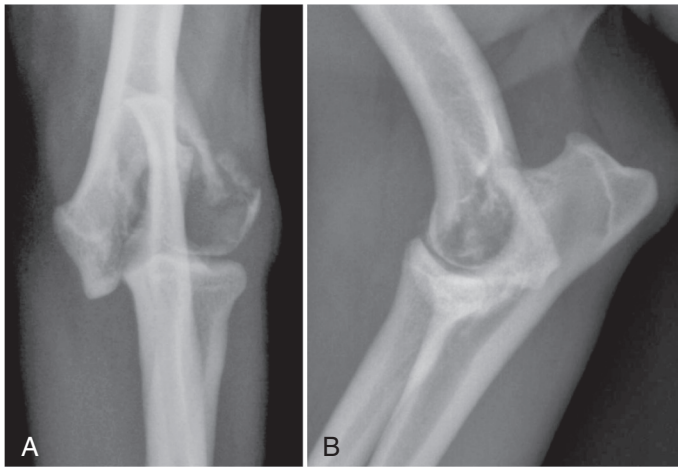

Fig. 21.63 Craniocaudal **(A)** and lateral **(B)** radiographs of a dog with extensive lysis of the lateral aspect of the humeral condyle. There is resulting pathologic fracture in the lateral epicondylar region, extending to involve the joint. Final diagnosis was diffuse mixed cell lymphoma of bone. (Courtesy of North Shore Veterinary Specialist Centre, Sydney, Australia.)

REFERENCES

1. Whiting PG, Pool RR: Intrameniscal calcification and ossification in the stifle joints of three domestic cats, *J Am Anim Hosp Assoc* 21:579, 1985.
2. Mahoney PN, Lamb CR: Articular, periarticular and juxtaarticular calcified bodies in the dog and cat: a radiologic review, *Vet Radiol Ultrasound* 37:3, 1996.
3. Mason DR, Schultz KS, Samii VF, et al: Sensitivity of radiographic evaluation of radio-ulnar incongruence in the dog in vivo, *Vet Surg* 31:125, 2002.
4. Widmer WR, Buckwalter KA, Braunstein EM, et al: Radiographic and magnetic resonance-imaging of the stifle joint in experimental osteoarthritis in dogs, *Vet Radiol Ultrasound* 35:371, 1994.
5. McGonagle D, Benjamin M, Marzo-Ortega H, et al: Advances in the understanding of entheseal inflammation, *Curr Rheumatol Rep* 4:500, 2002.
6. Morgan JP: *Radiology of skeletal diseases—principles of diagnosis in dogs*, Davis, CA, 1981, Veterinary Radiology Associates, p 22.
7. van Bree H: Vacuum phenomenon associated with osteochondrosis of the scapulohumeral joint in dogs: 100 cases, *J Am Vet Med Assoc* 201(1916):1992, 1985-1991.
8. *PennHIP training manual*, San Diego, CA, 1998, Synbiotics Corporation, p 22.
9. Hathcock JT: Vacuum phenomenon of the canine spine: CT findings in 3 patients, *Vet Radiol Ultrasound* 35:285, 1994.
10. Weber WJ, Berry CR, Kramer RW: Vacuum phenomenon in 12 dogs, *Vet Radiol Ultrasound* 36:493, 1995.
11. Rendano VT, Dueland R: Variation in location of gastrocnemius sesamoid bones (fabellae) in a dog, *J Am Vet Med Assoc* 173:200, 1978.
12. Freire M, Brown J, Robertson ID, et al: Meniscal mineralization in domestic cats, *Vet Surg* 39:545, 2010.
13. Walker M, Phalan D, Jensen J, et al: Meniscal ossicles in large non-domestic cats, *Vet Radiol Ultrasound* 43:249, 2002.
14. Muir P, Johnson KA: Supraspinous and biceps brachii tendinopathy in dogs, *J Am Anim Pract* 35:239, 1994.

15. Rivers B, Wallace L, Johnson GR: Biceps tenosynovitis in the dog: radiographic and sonographic findings, *Vet Comp Orthop Traumatol* 5:51, 1992.
16. Cake MA, Read RA: Canine and human sesamoid disease, *Vet Comp Orthop Traumatol* 8:70, 1995.
17. Read RA, Black AP, Armstrong SJ, et al: Incidence and clinical significance of sesamoid disease in rottweilers, *Vet Rec* 130:533, 1992.
18. Davis PE, Bellenger CR, Turner DM: Fractures of the sesamoid bones in the greyhound, *Aust Vet J* 45:15, 1969.
19. Ljunggren G, Olsson SE: Osteoarthrosis of the shoulder and elbow joints in dogs: a pathologic and radiographic study of necropsy material, *J Am Vet Radiol Soc* 16:33, 1975.
20. Innes JF, Costello M, Barr FJ, et al: Radiographic progression of osteoarthritis of the canine stifle joint: a prospective study, *Vet Radiol Ultrasound* 45:143, 2004.
21. Smith GK, Popovitch CA, Gregor TP, et al: Evaluation of risk factors for degenerative joint disease associated with hip dysplasia in dogs, *J Am Vet Med Assoc* 206:642, 1995.
22. Smith GK, Gregor TP, Rhodes WH, et al: Coxofemoral joint laxity from distraction radiography and its contemporaneous and prospective correlation with laxity, subjective score, and evidence of degenerative joint disease from conventional hip-extended radiography in dogs, *Am J Vet Res* 54:1020, 1993.
23. Marshall JL, Olsson SE: Instability of the knee: a long-term experimental study in dogs, *J Bone Joint Surg Am* 53:1971, 1561.
24. Lascelles BDX, Henry JB, Brown J, et al: Cross-sectional study of the prevalence of radiographic degenerative joint disease in domesticated cats, *Vet Surg* 39:535, 2010.
25. Hedhammar A, Olsson SE, Andersson SA, et al: Canine hip dysplasia: study of heritability in 401 litters of German shepherd dogs, *J Am Vet Med Assoc* 174:1012, 1979.
26. Hedhammar A, Wu FM, Krook L, et al: Overnutrition and skeletal disease, *Cornell Vet* 64:9, 1974.
27. Todhunter RJ, Grohn YT, Bliss SP, et al: Evaluation of multiple radiographic predictors of cartilage lesions in the hip joints of eight-month old dogs, *Am J Vet Res* 64:1472, 2003.
28. Lust G, Beilman WT, Dueland R, et al: Intra-articular volume and hip joint instability in dogs with hip dysplasia, *J Bone Joint Surg Am* 62:576, 1980.
29. Lust G, Beilman WT, Rendano VT: A relationship between degree of laxity and synovial fluid volume in coxofemoral joints of dogs predisposed for hip dysplasia, *Am J Vet Res* 41:55, 1980.
30. Morgan JP: Canine hip dysplasia: significance of early bony spurring, *Vet Radiol* 28:2, 1987.
31. Keller GG, Reed AL, Lattimer JC, et al: Hip dysplasia: a feline population study, *Vet Radiol Ultrasound* 40:460, 1999.
32. Smith GK, Biery DN, Gregor TP: New concepts of coxofemoral joint stability and the development of a clinical stress radiographic method for quantitating hip joint laxity in the dog, *J Am Vet Med Assoc* 196:59, 1990.
33. Gandolfi B, Alamri S, Darby WG, et al: A dominant TRPV4 variant underlies osteochondrodysplasia in Scottish fold cats, *Osteoarthr Cartil* 24:1441, 2016.
34. Ginja M, Caspar MR, Ginja C: Emerging insights into the genetic basis of canine hip dysplasia, *Vet Med Res Rep* 6:193, 2015.
35. Salter RB, Harris WR: Injuries involving the epiphyseal plate, *J Bone Joint Surg* 45:587, 1963.
36. Farrow CS: Stress radiography: applications in small animal practice, *J Am Vet Med Assoc* 181:777, 1982.
37. Davidson EB, Griffey SM, Vasseur PB, et al: Histopathological, radiographic, and arthrographic comparison of the biceps tendon in normal dogs and dogs with biceps tenosynovitis, *J Am Anim Hosp Assoc* 36:522, 2000.
38. Grundmann S, Montavon PM: Stenosing tenosynovitis of the abductor pollicis longus muscle in dogs, *Vet Comp Orthop Traumatol* 14:95, 2001.
39. Kramer M, Stengel H, Gerwing M, et al: Sonography of the canine stifle, *Vet Radiol Ultrasound* 40:282, 1999.
40. Crawley AC, Yogalingam G, Muller VJ, et al: Two mutations within a feline mucopolysaccharidosis type VI colony cause three different phenotypes, *J Clin Invest* 101:109, 1998.
41. Malik R, Allan GS, Howlett CR, et al: Chondro-osseous dysplasia in Scottish fold cats, *Aust Vet J* 76:85, 1998.
42. Bellah JR, Weigel JP: Hemarthrosis secondary to suspected warfarin toxicosis in a dog, *J Am Vet Med Assoc* 182:1126, 1983.
43. Bennett D, Taylor DJ: Bacterial infective arthritis in the dog, *J Small Anim Pract* 29:207, 1988.
44. Moise NS, Crissman JW, Fairbrother JF, et al: *Mycoplasma gateae* arthritis and tenosynovitis in cats: case report and experimental reproduction of the disease, *Am J Vet Res* 44:10, 1983.
45. Bennett D: Immune-based erosive inflammatory joint disease of the dog: canine rheumatoid arthritis: I. Clinical, radiological and laboratory investigations, *J Small Anim Pract* 28:779, 1987.
46. Pedersen NC, Pool RR, O'Brien T: Feline chronic progressive polyarthritis, *Am J Vet Res* 41:522, 1980.
47. Bennett D: Immune-based non-erosive inflammatory joint disease of the dog: I. Canine SLE, *J Small Anim Pract* 28:871, 1987.
48. Moise NS, Crissman JW: Chronic progressive polyarthritis in a cat, *J Am Anim Hosp Assoc* 18:965, 1982.
49. Bennett D, Nash AS: Feline immune-based polyarthritis: a study of thirty-one cases, *J Small Anim Pract* 29:501, 1988.
50. Marti JN: Bilateral pigmented villonodular synovitis in a dog, *J Small Anim Pract* 38:256, 1997.
51. Hanson JA: Radiographic diagnosis—carpal villonodular synovitis, *Vet Radiol Ultrasound* 39:15, 1998.
52. Flo GL, Stickle RL, Dunstan RW: Synovial chondrometaplasia in five dogs, *J Am Vet Med Assoc* 191:1417, 1987.
53. Hubler M, Johnson KA, Burling RT, et al: Lesions resembling osteochondromatosis in two cats, *J Small Anim Pract* 27:181, 1986.
54. Vail DM, Powers BE, Getzy DM, et al: Evaluation of prognostic factors for dogs with synovial sarcoma: 36 cases (1986-1991), *J Am Vet Med Assoc* 205:1300, 1994.
55. Silva-Krott IU: Synovial sarcoma in a cat, *J Am Vet Med Assoc* 203:1430, 1993.
56. McGlennon NJ, Houlton JEF, Gorman NT: Synovial sarcoma in the dog—a review, *J Small Anim Pract* 29:139, 1988.
57. Whitelock RG, Dyce J, Houlton JEF, et al: A review of 30 tumours affecting joints, *Vet Comp Orthop Traumatol* 10:146, 1997.

ELECTRONIC RESOURCES

evolve

Additional information related to the content in Chapter 21 can be found on the companion Evolve website at: http://evolve.elsevier.com/Thrall/vetrad/

- Chapter quiz